Check for updates

Small lectin ligands as a basis for applications in glycoscience and glycomedicine†

Paul V. Murphy, [ID] *[abc] Ashis Dhara, [ID] [ab] Liam S. Fitzgerald, [ID] [abc] Eoin Hever,[a] Saidulu Konda [ID] [a] and Kishan Mandal[a]

Glycan recognition by lectins mediates important biological events. This Tutorial Review aims to introduce lectin–ligand interactions and show how these molecular recognition events inspire innovations such as: (i) glycomimetic ligands; (ii) multivalent ligand agonists/antagonists; (iii) ligands for precision delivery of therapies to cells, where therapies include vaccines, siRNA and LYTACs (iv) development of diagnostics. A small number of case studies are selected to demonstrate principles for development of new ligands for applications inspired by knowledge of natural glycan ligand structure and function.

Key learning points
- Introduction to glycan and glycoconjugate structure.
- Factors influencing ligand–lectin interactions.
- Principles for glycomimetic research.
- Principles for multivalent ligand design to increase avidity and selectivity.
- Applications in chemical biology, biomedical science.

1. Introduction

Glycans are mostly found on cell surfaces of organisms. These carbohydrates are conjugated to proteins (glycoproteins) and lipids (glycolipids). Glycoconjugate-protein recognition modulates biological events including cell adhesion, disease progression, immunological responses and infection.[1] Lectins are one of two distinct classes of glycan binding proteins, the second being proteins that bind sulfated glycosaminoglycans. Lectins are classified into evolutionarily related families identified by carbohydrate-recognition domains (CRDs) based on primary and/or three-dimensional structural similarities. Lectins typically recognize terminal groups on glycan ligands, which fit into CRDs.[2] Multivalency occurs, when multiple copies of ligands are found on natural scaffolds, as for glycans on surfaces. Lectins are often also multimeric, which results from either noncovalent or covalent association of two or more monomers with CRDs. Interaction between multimeric lectins and multimeric ligands gives more avid interaction.[3] Ligand lectin recognition is central to the sugar code in biology (Fig. 1).[4]

This Tutorial Review focuses on three small lectin ligand types: natural glycan ligands; glycomimetics and glycocluster ligands. We provide knowledge of glycan structure (Section 2) and features of their interaction with lectins.[5] Design of bioavailable glycomimetic ligands (Section 3) and small glycoclusters (Section 4) with biomedical or chemical biological applications are emerging from research. We have selected case studies to demonstrate how novel lectin ligand inhibitors are being developed, including some that are entering or have entered clinical trials. We discuss how research on lectin ligands is leading to innovations enabling precision delivery of vaccines and short interfering RNA (siRNA) to cell types and for chemical biology or sensing applications based on glycoclusters.

2. Natural glycans and interaction with lectins

2.1 Introduction to glycans

Mammalian cell surface glycans (Fig. 2),[6] are comprised of monosaccharides in pyranose forms (Fig. S1, ESI†), including

[a] School of Biological and Chemical Sciences, Galway, H91TK33, Ireland.
 E-mail: paul.v.murphy@universityofgalway.ie
[b] SSPC, SFI Research Centre for Pharmaceuticals, Galway, H91TK33, Ireland
[c] CÚRAM, SFI Research Centre for Medical Devices, University of Galway, University Road, Galway, H91TK33, Ireland
† Electronic supplementary information (ESI) available: Figures and tables. See DOI: **https://doi.org/10.1039/d4cs00642a**

9428 | *Chem. Soc. Rev.*, 2024, **53**, 9428–9445

This journal is © The Royal Society of Chemistry 2024

mannose (Man), galactose (Gal) or *N*-acetylgalactosamine (GalNAc), *N*-acetylglucosamine (GlcNAc), fucose (Fuc) and *N*-acetylneuraminic acid or sialic acid (NeuAc). Herein it is assumed that abbreviations such as Gal, GalNAc refer to the more common pyranose form unless otherwise stated (*e.g.* Man = mannopyranose, Man*s* = mannoseptanose). The position of linkage between saccharides and anomeric configuration generated by glycosyltransferases influences the properties of glycans produced, including their interaction with lectins.

2.2 Pyranose ring conformation is influenced by steric interactions and torsional strain

Pyranoses adopt chair conformations (Fig. S4, ESI†) to minimise strain with most substituents equatorial to minimise steric repulsive interactions; this, for example, gives the $^4C_1$ conformation for Gal depicted in Fig. 2 and Fig. S4A (ESI†); its $^1C_4$ conformer has both destabilising 1,3-diaxial interactions and Hassel-Ottar (1,3-syndiaxial or *syn*-pentane) interactions. The boat is not preferred as it displays torsional strain.

2.3 The *exo*-anomeric effect influences conformation

The α- and β-D-glucopyranoses are the main populated forms for glucose in water and are in equilibrium and a preference is observed for β-D-Glc (equatorial OH at C-1). However, there is ∼3-fold increase for the OH group at C-1 in Glc to be axial compared to cyclohexanol; this increased preference for the axial anomer is the original definition of the *endo*-anomeric effect.[7]

The *endo*-anomeric effect[9] is stereoelectronic, requiring an electron withdrawing heteroatom (O-5) in the ring and an electron withdrawing atom (O-1) at C-1. One model proposed to explain the *endo*-anomeric effect is hyperconjugation (Fig. S2, ESI†), possible when the anomeric substituent is axial, but, not when equatorial. Another proposal to explain the effect is based on minimisation of electrostatic repulsion between oxygen atoms. Explaining anomeric preference is, however, more complex and influenced by multiple factors[10] such as solvent, and the extent of steric repulsions, which are reduced by electron withdrawing substituents.[11] The *endo*-anomeric effect gives rise to the *exo*-anomeric effect (Fig. S3, ESI†), which is considered
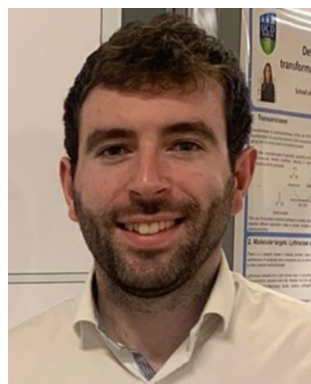
Paul V. Murphy

Paul Murphy received his BSc and PhD from University College Galway of the National University of Ireland. After appointment as a Chiroscience Postdoctoral Fellow at University of York, UK, he was appointed as a Lecturer and later as an Associate Professor in Organic Chemistry at University College Dublin and subsequently as an Established Professor of Chemistry at the University of Galway. His research interests are now focused on design and synthesis of glycomimetics and glycoclusters and includes synthesis method development for carbohydrate chemistry.

Ashis Dhara

Ashis Dhara received an MSc degree in Chemistry from Dr Shakuntala Misra National Rehabilitation University, India. He earned his PhD in 2024 from the University of Galway, Ireland, supervised by Professor Paul V. Murphy. Currently, he is a Postdoctoral Researcher in the Science Foundation Ireland Research Centre for Pharmaceuticals (SSPC) at University of Galway. His research focuses on design, synthesis, and evaluation of glycomimetics as lectin inhibitors.

Liam S. Fitzgerald

Liam Fitzgerald obtained his BSc from Maynooth University in 2018. Afterwards he pursued a PhD at the University of Galway supervised by Dr Miriam O'Duill and Prof. Paul Murphy and graduated in 2023. During this time, he worked on developing methodology for deuterating indoles as well as the development of multivalent sialic acid derivatives as inhibitors of influenza hemagglutinin. He will shortly begin work as a postdoctoral research fellow at the Krembil Research Institute with Prof. Donald Weaver.

Eoin Hever

Eoin Hever received BSc and MSc (Research) degree from National University of Ireland Galway. Eoin subsequently completed his PhD research at University of Galway under the supervision of Professor Paul Murphy in 2023. Eoin's research focused on the design and synthesis of novel constrained glycomimetics as inhibitors of galectins and galactosidases. During the PhD he had research visits to University of Copenhagen and University of Lund, the latter supported by an EMBO travel award. Eoin is now working as a Research Chemist in Merck Sharp & Dohme, Ireland.
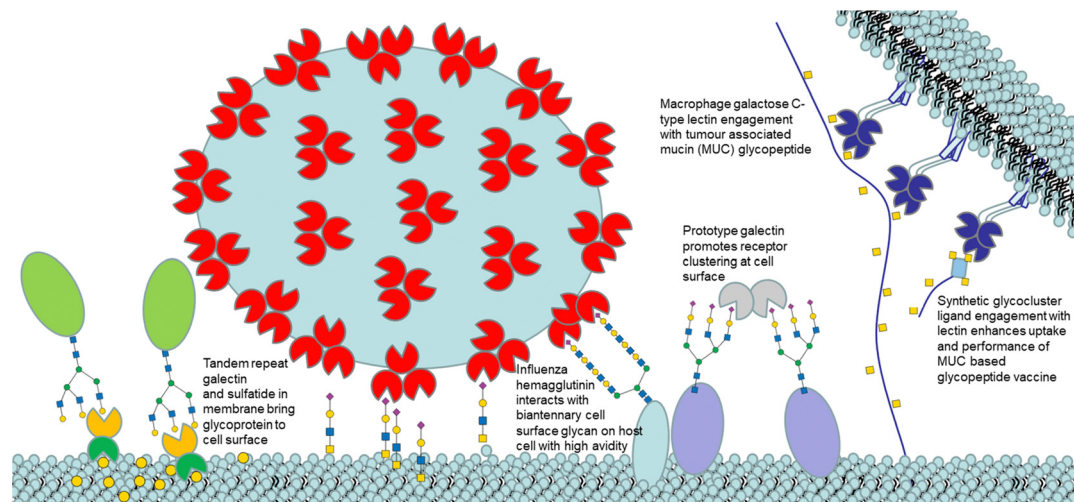
Fig. 1 Cartoon illustration (not to scale) of selected lectin ligand mediated events at a cell surface.

when accurately calculating energies of ligand conformers that interact with lectins.

2.4 The *gauche* effect and conformation

The *gauche* effect[12] is a stereoelectronic based increase in the preference for the *gauche* arrangement of F, and to a lesser degree, of O substituents on adjacent carbon atoms and is thus relevant to carbohydrates, particularly the ω torsion in 1,6 disaccharide and related linkages (Fig. S5, ESI†).

2.5 Interglycosidic torsion preferences determine glycan conformation

The 3D structure of glycans is determined primarily by the conformational preferences of the bonds between saccharide residues (interglycosidic torsions, Φ, Ψ, ω), influenced by the exoanomeric effect, *gauche* effect and steric factors. The topic has been reviewed.[13] Disaccharide conformation based on crystal structure data of glycans bound to proteins/antibodies, collected by Wormwald and co-workers provides experimentally derived information, which includes $\Phi-\Psi$ and $\Phi-\Psi-\omega$ plots.[14] Woods's glycam.org is a reliable source of low energy structures of glycans.[15] We provide additional notes and Fig. S3–S8 (ESI†) on glycan conformation in the ESI† file as well as selected energy surface plots reproduced from literature sources in Fig. S9–S12 (ESI†).[16]

2.5.1 Case study: structure of lactose. NMR study from Jiménez-Barbero and co-workers of lactose in water indicated 75–97% population of the *exo-syn* Φ and *syn-*Ψ[17] conformer

Saidulu Konda was born in Telangana, India (1985), and is currently Senior Chemist at Arran Chemical Company, Athlone (Ireland). He received his BSc from Osmania University in 2007 and MSc in Organic Chemistry from M.N.R. P.G. Collage (Affiliated to Osmania University) in 2010. He got his PhD in Stereoselective Synthesis of C27-C35 Eribulin Fragment and Related Macrocycles, at the University of Hyderabad (UGC Research Fellow)

Saidulu Konda

in 2015 under the supervision of Professor Prabhat Arya. After four years (2016–2020) industrial experience in GVK Biosciences, Bengaluru he was appointed as a postdoctoral researcher for three years (2020–2023) supported by SFI and the Irish Research Council at NUI Galway under the supervision of Professor Paul Murphy. His research interests are (i) the synthesis of natural product-inspired macrocycles, (ii) total synthesis of natural products, and (iii) carbohydrate research.

Kishan Mandal

Kishan Mandal was awarded his BSc in Chemistry from Burdwan University, India, in 2015, and his MSc in Organic Chemistry from DHSGSU, India, in 2017. He worked in the laboratory of Dr Chandan K. Jana at IIT Guwahati, India, as a Junior Research Fellow from February 2019 to June 2019, focusing on the total synthesis of bioactive natural products. Currently, he is pursuing his PhD under the supervision of Prof. Paul Murphy at the University of Galway, Ireland. His research is centred around the design and synthesis of new inhibitors of galectins and siglecs.
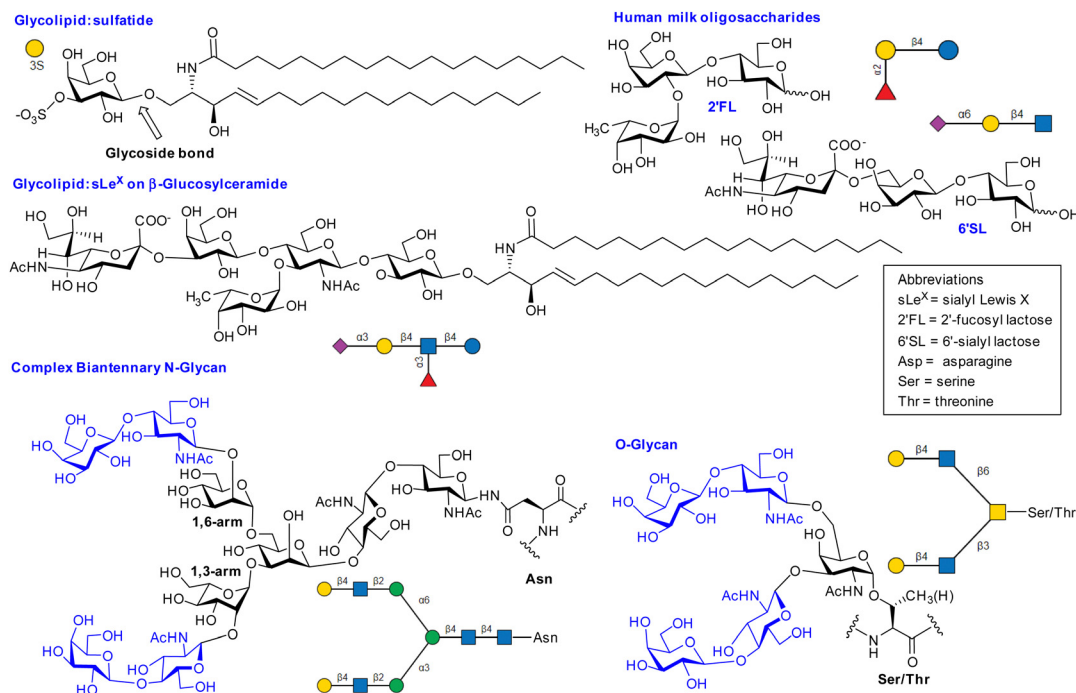
9430 | *Chem. Soc. Rev.*, 2024, **53**, 9428–9445

This journal is © The Royal Society of Chemistry 2024

Fig. 2 Selected examples of lectin ligands. SNFG nomenclature was generated using glycoglyph.[8] The *N*-glycan and *O*-glycans shown are bivalent glycoclusters where two LacNAc disaccharides (blue) are presented on saccharide scaffolds (black).

with minor population of *exo-syn Φ* and *anti-Ψ* (∼3–25%), and with no evidence of population of other conformers. The latter analysis was based on favourable comparison between residual dipolar coupling measurement and molecular dynamics (MD) simulations, which gave *Φ* and *Ψ* of 49° and 13° for the major conformer, which agreed well with lactose's crystal structure geometry.[18]

2.5.2   Case study: structure of Manα1,6Man. MD simulations and NMR spectroscopy showed[19] that the glycosidic torsion preferences for Manα1,6Man in water were: (i) *exo-syn-Φ*; *anti-Ψ* (Fig. S4E, ESI†); *ω* was ∼50:50 *gg* and *gt* conformers, accounting for ∼95% of all *ω* torsion conformers.

2.6   What glycan conformation is recognised by a lectin?

The conformation of a ligand bound to the lectin CRD may be similar to that determined in the gas phase, in solution or in crystal structures.[20] Summarised in Table S1 (ESI†) are the glycosidic torsions observed in a subset of crystal structures, where lactose or its derivatives are bound to various galectin CRDs; the bound ligands all have the *exo-syn Φ* and *syn-Ψ* conformation, which is like unbound lactose conformers observed in gas/solution/solid state.

There is evidence also for multiple modes of binding, where lectins recognise different ligand conformers, which arise if multiple conformers are populated. The interaction between a Manα1-3Man and rat mannose binding protein (rMBP) was studied by NMR spectroscopy and MD.[21] The unbound Manα1-3Man showed population of two conformers, where the interglycosidic torsions were: (i) *exo-syn Φ* and *syn-Ψ* and (ii)

exo-syn Φ and *anti-Ψ* and the two conformers were detected to bind to rMBP.

Induced fitting of lectin may occur on binding, and ligand conformer selection is known.[22] One interesting example of induced fitting is in catch bonding. Catch bonds are biological interactions that are enhanced by mechanical force and occur when protein–ligand binding mode changes, due to conformational changes, leading to altered affinity. Catch bonding is associated with cell–cell adhesion under shear stress.

2.6.1   Catch bonding in FimH–Man interaction. FimH is a bacterial adhesin that recognises Man containing glycans and is associated with urinary tract infection. FimH is a two-domain protein, composed of an N-terminal lectin domain (FimH$_{LD}$) and a C-terminal pilin domain (FimH$_{PD}$). Binding of small ligands by FimH[23] is influenced by allostery where FimH$_{PD}$ induces a low affinity open shallow CRD conformation. Under conditions of shear stress,[24] however, allostery is switched off, the lectin domain adopts a closed deep conformation,[25] which binds the ligand more tightly; this conformational change plays a key role in maintaining bacterial adhesion to Man containing glycans on kidney cells under shear stress associated with urine excretion. The FimH$_{LD}$ in the closed conformation shows high affinity for mannose with K_d 1.672 ± 0.094 μM (ITC),[26] whereas the K_d for the open conformation to bind mannose is only 0.32 ± 0.02 mM[27] showing the importance of binding site shape (shallow vs deep) in influencing affinity in lectin–ligand interaction.

2.6.2   Catch bonding in selectin–ligand interaction. Le^X is typically found on leukocyte and other cell surface glycolipids

This journal is © The Royal Society of Chemistry 2024

Chem. Soc. Rev., 2024, **53**, 9428–9445 | **9431**

(Fig. 2) or glycoproteins and its interaction with E-selectin contributes to cell–cell adhesion during the inflammatory/immune response.[28] Several E-selectin-sLe^X crystal structures have been reported and different binding modes have been observed after (i) soaking E-selectin crystals with sLe^X (PDBID: 1G1T)[29] and (ii) co-crystallisation with sLe^X (PDBID: 4CSY).[30] MD simulations predicted that E-selectin has a higher affinity for sLe^X by 0.82 kcal mol^{-1} in the 4CSY structure *versus* that of 1G1T, which corresponds to a ∼4-fold affinity enhancement for the co-crystallisation induced complex. This higher affinity binding mode is induced under conditions of shear force, where the lifetime of sLe^X-selectin complex is increased, with this sustaining attachment and rolling of neutrophils and other immune cells on blood vessels, as part of the immune response.

2.7 Non-covalent interactions in lectin ligand complexes

Hydrogen bonding of saccharide hydroxyl groups, including water mediated H-bonding between ligand and lectin is prevalent. For NeuAc containing glycans, there is frequently salt bridging or charged–charged or charged–neutral H-bonding to arginine, interactions which also occur for sulfated glycans. Hydrophobic interactions and/or CH–Pi interactions[31] are frequently involved. Ligand hydroxyl groups can coordinate to metal ions (*e.g.* Ca^{2+}) which induce charge transfer interactions from saccharide to metal ion.[32] Fig. S3–S5 (ESI†) shows interactions in selected complexes between ligands and lectins. Fig. S3 (ESI†) shows the interaction of sulfatide with galectin-8, with recent crystallographic evidence showing that sulfatide sphingosine residue's hydroxyl group has indirect water mediated H-bonding interaction with the N-terminal domain;[33] this shows contribution to lectin–ligand interaction of the sphingosine component of the glycolipid and contributes to understanding how sulfatide recognises lectins. We discuss below the full ligand for P-selectin, which is a glycosulfopeptide of the P-selectin glycoprotein ligand (PSGL). Thus, lectin–ligand recognition does not always involve only the glycan residue.

2.8 Thermodynamics of lectin–ligand interaction

Low affinity lectin–monosaccharide interactions are prevalent, and a contributing factor is that the binding pocket (CRD) is often shallow, with a substantial area of bound ligand surrounded by solvent water, contributing to a relatively high dielectric constant, ε, for the CRD. Coulomb's law implies the force between electrostatic based interactions, which include H-bonding,[34] is weaker in a pocket with higher ε and this increases K_d or reduces affinity. Higher affinity can arise where pockets are deeper and have lower ε as for FimH in its high affinity binding conformation as occurs in catch bonding. Ernst and co-workers indicate[35] the strength of a H-bond could increase by ∼10 fold in a pocket with ε = 5–10 compared to one with ε = 20. Another feature is that K_d depends upon ligand binding on and off rates ($K_d = k_{off}/k_{on}$). It is easier for a ligand to dislodge from a shallow pocket than from an enclosed one and, thus, k_{off} is reduced in the deeper pocket, reducing K_d.

The binding free energy ($-\Delta G$) increases (K_d reduces) as affinity increases, when comparing ligands and it has

contributions from enthalpy ($-\Delta H$) and entropy ($+T\Delta S$) according to the equation $-\Delta G = -\Delta H + T\Delta S$. Ligand binding is often enthalpy driven with the entropy change usually unfavourable, although there are exceptions such as for the sLe^X-E-selectin interaction.[36]

Increasing $-\Delta H$ is associated with stronger interactions or extended site interactions, although it could be reduced if the binding mode must adopt an energetically less favourable conformation. Extended site interactions arise, for example, for a larger oligosaccharide binding to a lectin, when compared to a monosaccharide.[37]

It has been proposed that when performing research to optimise ligand affinities, required during drug discovery, to focus on measuring or computing free energies of protein–ligand interactions, rather than trying to solely focus on improving enthalpy or entropy alone, as enthalpy–entropy compensation can frustrate ligand design.[38]

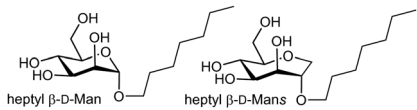### 2.8.1 Case study – dissection of entropy contributions to ΔS in FimH–ligand binding

The entropy contribution to the free energy of binding is a sum of changes in translational, rotational, conformational, and solvation entropies. A study by Peczuh, Ernst and co-workers provides an informative analysis of various entropy contributions in the binding of monosaccharide ligands to the high affinity state of FimH.[39]

Conformational entropy, due to induced fitting, results from a ligand and/or lectin reorganising from a non-binding to binding conformation. The degree to which reorganisation takes place influences the magnitude of ΔS and is unfavourable entropically and reduces $-\Delta G$. Two high affinity ligands for FimH, heptyl β-D-Man, and a septanoside, heptyl β-D-Man$s$, were studied, with ITC investigation indicating the difference in K_d ($\Delta\Delta G$ = 5.5 kJ mol^{-1} or ∼1.3 kcal mol^{-1}) between the two ligands is mainly due to $T\Delta S$ (see Table 1).

Metadynamics simulations showed that the septanoside's ring is more flexible than of heptyl β-D-Man. The crystal structures of both ligands with FimH revealed identical H-bonding networks in their interaction, consistent with near identical enthalpy change measured for the two ligands. There is a conformation difference when orientation of heptyl groups is compared in the two co-crystal structures, but DFT calculations indicated that the binding energy contribution by the heptyl groups are equivalent in both crystal structures and that only one of the septanoside ring conformers is bound by the lectin. The $T\Delta S$ due to losses in rotational and translational entropy on binding were considered equal in both cases (−10 kJ mol^{-1}). The authors concluded that the entropy difference is associated with either solvation or conformational entropy. ITC measurements at different temperatures revealed almost identical ΔC_p values for both ligands, which enabled establishment that the desolvation entropies ($+T\Delta S_{solv}$ = +69.1 kJ mol^{-1} & +68.8 kJ mol^{-1}) are nearly identical for the two ligands. The authors concluded that the difference in conformational entropy ($+T\Delta S_{conf}$ = +66.4 kJ mol^{-1}) for heptyl β-D-Man *vs.* +70.6 kJ mol^{-1} for heptyl β-D-Man$s$ accounts for

9432 | Chem. Soc. Rev., 2024, 53, 9428–9445

This journal is © The Royal Society of Chemistry 2024

Table 1 Data for binding of ligands to FimH

heptyl β-D-Man   heptyl β-D-Man*s*

Ligand	K_d (nM)	$-\Delta G$ (kJ mol^{-1})	$-\Delta H$ (kJ mol^{-1})	$+T\Delta S$ (kJ mol^{-1})
heptyl β-D-Man	29 (25.8–32.3)	+43.0	+50.3 (+50.2 to +50.7)	−7.3
heptyl β-D-Man*s*	264 (245–284)	+37.5	+49.4 (+48.9 to +49.8)	−11.8

most of the 10-fold difference in affinity ($\Delta\Delta S_{conf}$ = 4.2 kJ mol^{-1}, $\sim$1.0 kcal mol^{-1}).

3. Glycomimetic ligands for galectins, selectins and siglecs

For drug discovery, substances that maintain a therapeutic concentration over an extended period, metabolic stability, and slow and prolonged renal excretion are required,[40] however, these requirements are usually not met by natural glycan ligands, but may be met by synthetic mimics or glycomimetics, which requires acquiring fundamental knowledge of lectin–ligand interaction, such as identification of the key groups involved in interactions and 3D structure.[41,42] High affinity ligands, ideally with $K_d \sim$ 50 nM or lower, is desired for drug discovery projects along with good selectivity profile for the lectin of interest. Oral bioavailability for glycomimetics is desired but is not essential. The development of glycomimetic drugs, substances that are clinically approved by regulatory bodies, has been relatively slow compared to other types of drugs. Tamiflu, although not a lectin inhibitor, is an exemplar synthetic glycomimetic,[43] which gained regulatory approval as a drug. Tamiflu is a glycosidase (neuraminidase) inhibitor, for therapy or prevention of influenza infection. Tamiflu's development started from 2,3-dehydro-2-deoxy-NeuAc, which is a mimetic of the transition state of the neuraminidase catalysed reaction. One lesson from Tamiflu's development was that the systematic elimination of polar groups and their replacement with a more lipophilic group did not compromise affinity. Oral bioavailability was achieved by esterification of the acid group to give a lipophilic prodrug. A general strategy employed by medicinal chemists in lectin ligand development, is to identify core structural features in the native ligand essential for lectin recognition with subsequent removal of unnecessary polar groups, while appending groups capable of additional interactions or give desired pharmacological properties. Such approaches have, in recent years, yielded candidates that have entered clinical trials as E-selectin and galectin-3 inhibitors.

3.1 Glycan ligands for galectins

Galectins[44] are tissue lectins, of which 15 mammalian members are known, that play roles in cancer and inflammation and they generally bind β-galactopyranosides.[45] There are three types of galectin: prototype (*e.g.* galectins-1,7), chimeric (galectin-3) and tandem repeat (*e.g.* galectin-4,8,9). Tandem repeat galectins have two unique CRDs, referred to as the N and C-terminal domain, separated by a covalently bound peptide linker. The CRDs have a conserved β-sandwich core sequence containing $\sim$130 amino acids which contains a groove long enough to hold a linear tetrasaccharide. Binding of the galactopyranoside within the galectin CRD's groove is the most conserved feature of ligand recognition and includes cooperative H-bonding of the 4-OH and 6-OH with His, Arg and Asp residues; there are CH–Pi interactions of the α-face of Gal with Trp. Lactose is considered a minimal ligand with affinity in the mM range,[46] although binding has been detected for some galectins at mM or high mM concentrations for simpler galactopyranosides (see Table S2, ESI†). The various galectins bind lactose's *exo-syn-Φ/syn-Ψ* conformer. For some galectins, the affinity is increased for LacNAc derivatives compared to lactose with extended site interaction involving the acetamide explaining this. Gal-8,[47] shows high affinity (2.7 μM, from SPR) for 3-O-sialylated lactose compared to LacNAc (type 1 or 2) or lactose (79–420 μM), with the increased affinity due to the interaction of the NeuAc carboxylate with sidechains of Arg59 and Gln47 in the N-terminal CRD (Gal-8N).[48] Thus while galectins minimally recognise β-galactopyranosides, the affinity and selectivity varies between different galectins for different glycans, with synthesis being used to develop more potent glycomimetic ligands.

3.2 Glycomimetics for galectins

Nilsson *et al.* generated 3′-amino-LacNAc, where the galactopyranoside 3-OH is replaced with an amino group and subsequent amide synthesis from the amino group led to the *p*-methoxytetrafluorobenzamide, which was $\sim$50-fold more potent than LacNAc; this showed the benefit from modifying galactopyranoside's 3-position.[49] Nilsson and co-workers later synthesised 3-substituted derivatives of thiodigalactoside (TDG, Fig. 3). TDG was first synthesised more than 100 years ago[50]
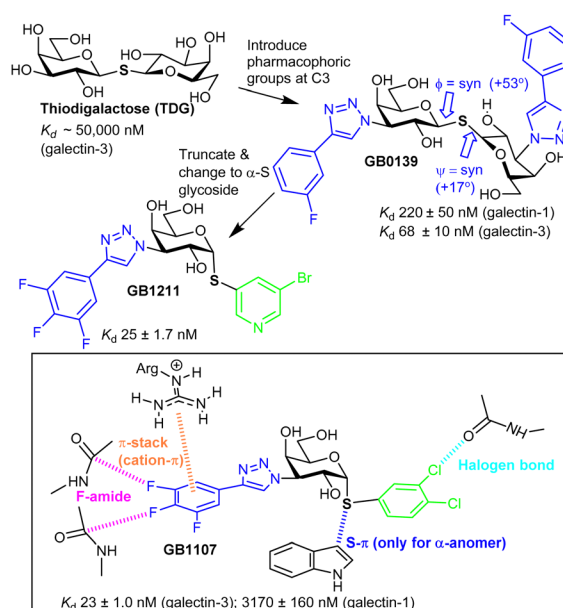

Fig. 3 Evolution of galectin glycomimetic ligands.

This journal is © The Royal Society of Chemistry 2024

Chem. Soc. Rev., 2024, **53**, 9428–9445 | 9433

and is stable to the action of galactosidases due to its *S*-glycoside and, thus, has bioavailability. TDG inhibits several galectins[51] (Table S2, ESI†) with higher affinity than lactose/LacNAc; it has similar affinity for galectin-1 and galectin-3 and has proven to be useful for study of their biological function.[52]

TDG has a $K_d \sim$ 50 μM for galectin-3, and subsequent replacement of its two 3-OH groups with aryltriazoles led to GB1039,[53] with a much improved K_d, 68 ± 10 nM.[54] *S*-Glycosidic linkages may have more flexibility than an *O*-glycoside,[55] yet, galectin-3 selects a conformer of GB1039 with an inter-residue torsion profile similar to lactose.[56] GB0139 entered clinical trials as an inhaled, not orally available, inhibitor of idiopathic pulmonary fibrosis.[57] However the GB1039's Phase 2b trial was not successful and Galecto, Inc. have since discontinued its development.[58] Research inspired by GB1039 has, however, led to discovery of GB1211[59,60] and GB1107, which are both orally available. GB1211 is a nM range inhibitor, with selectivity for galectin-3 and its affinity is explained by interactions like those shown in Fig. 3 for GB1107.[61] The cell permeability of GB1211 is linked to its lower polar surface area, when compared to GB1039 (114 *vs.* 201 Å²). GB1121 has a better safety profile than GB1107 and Galecto, Inc. are now pursuing clinical evaluation of GB1121 for oncology and liver fibrosis.

3.3 Selectin glycomimetic ligands

P-, E- and L-selectin are glycoprotein receptors that are involved in adherence and subsequent rolling of leukocytes on endothelium during inflammation or immune response before their secure attachment and recruitment into tissues and sLe^X is a minimal glycan ligand for the selectins. There have been sustained efforts over 30 years to develop pharmacologically effective sLe^X mimetics.

The binding of sLe^X to E-selectin is dependent on bidentate coordination of L-fucopyranoside to Ca^{2+} and interaction of NeuAc's carboxylate with Tyr and Arg. sLe^X is preorganised into its bioactive conformation with high and low affinity binding modes identified (Section 2.5.2 above).[62] Interaction of sLe^x to E-selectin is enthalpically unfavourable and entropically driven ($-\Delta H = -5.4 \pm 0.7$ kJ mol^{-1}, $+T\Delta S = +23 \pm 1$ kJ mol^{-1}).

Regarding P-selectin, a high affinity natural ligand has been identified, PSGL-1. PSGL-1 is a homodimeric transmembrane protein that presents sLe^X and sulfated tyrosine residues. The soluble recombinant form of PSGL-1 has a K_d value for P-selectin of $\sim$800 nM, which has much higher affinity than sLe^X alone (K_d = 7.8 mM). The affinity of PSGL-1 compared well to that of a truncated sulfated glycopeptide derived from the PSGL1, presenting the sLe^X and three sulphated tyrosine residues. Crystal structure of the glycosulfopeptide ligand bound to P-selectin showed interactions of the sulfate groups with Arg85 and His114, residues not replicated for E-selectin, explaining the increased affinity of PSGL-1 for P-selectin.[63]

Knowledge regarding ligand–selectin interactions have informed glycomimetic development. Binder, Ernst, and co-workers reported mimetics BEM1 and BEM2 (Fig. 4), where the NeuAc residue is replaced by the *S*-cyclohexyl lactate group and the GlcNAc residue is replaced by a substituted cyclohexane.
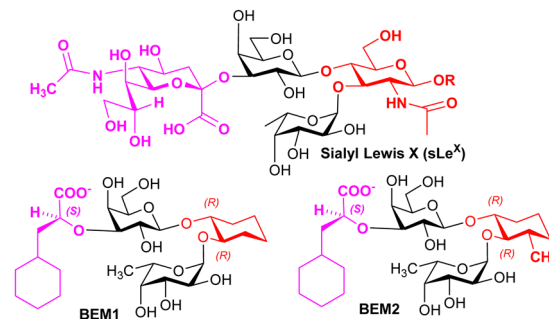

Fig. 4 Structures of sLe^X and mimetics.

The main purpose of the *S*-cyclohexyl lactate is to ensure optimal conformational preorganisation of the carboxylate group, relative to that of the L-Fuc for binding; the use of the *R*-cyclohexyl lactate produces a conformation that is not pre-organised correctly. Preorganisation of ligand pharmacophoric groups correlates with affinity for E-selectin.[64] BEM2 showed a K_d (ITC) of 19 ± 2 μM for E-selectin compared to 878 ± 93 μM (ITC) for sLe^X, whereas BEM1 was $\sim$3-fold less potent than BEM2. When compared with sLe^X, the affinity gain for BEM2 is almost entirely due a more favourable enthalpic contribution, while showing a similar entropic contribution observed for sLe^X. The major difference between BEM1 and BEM2 is in the entropy contribution, which we speculate may be linked to more flexibility in the cyclohexane in BEM1, reduced by the additional methyl substituent in BEM2.

Based on their observations, Ernst, Binder and co-workers proposed that glycomimetic design should involve replacing glycan components with predominantly structural (scaffold) roles with hydrophobic groups that can mimic the same structural role, to improve the enthalpic contributions to binding while reducing solvation penalties;[65] this assumes that the glycan component being replaced has purely a scaffolding role with no important interaction with the lectin. This very important finding informs strategy to contribute to optimising free energy of binding of glycomimetics. Co-crystallisation of BEM2 with E-selectn (PDB = 4C16) enabled confirmation of the structural role for the cyclohexane.[66] Furthermore, ligands for E-selectin with low nM range affinity have been synthesised, incorporating groups that introduce binding at a second site.[67]

3.4 Rivipansel and Uproleselan

Rivipansel,[68] and Uproleselan are sLe^x mimetics containing the essential minimal pharmacophoric groups for selectin recognition (Fig. 5), and both contain features found in the BEM2 glycomimetic. In Rivipansel, sulfate groups were incorporated with the aim to generate an improved L- and P-selectin ligand. Thus, Rivipansel is as a pan-selectin inhibitor and it showed increase in affinity for all three selectins compared to sLe^X. Nevertheless, evidence indicates Rivipansel's effectiveness is linked to selective inhibition of E-selectin; in an ELISA involving immobilised selectins, was >78-fold better ($\sim$4.3 μM) for E- than P- (423 μM) and L-selectin (337 μM). Also, Rivipansel inhibited E-selectin mediated rolling in a flow chamber cell-

9434 | *Chem. Soc. Rev.*, 2024, **53**, 9428–9445

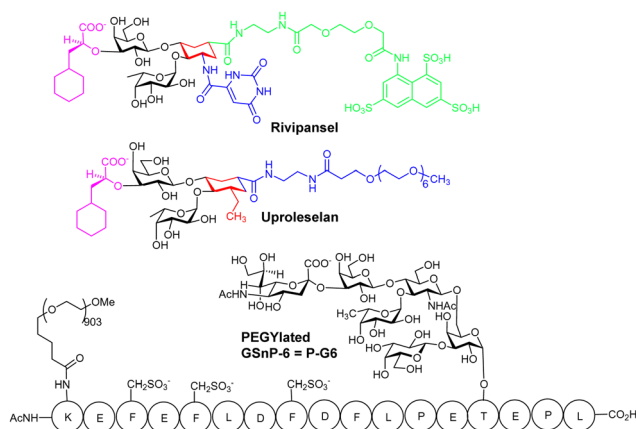This journal is © The Royal Society of Chemistry 2024

Fig. 5 Structures of Rivipansel, Uproleselan and P-G6. Amino acids are shown in single letter code form. $Tyr-OSO_3^-$ in PSGL-1 are replaced with $CH_2SO_3^-$ groups to get G-SnP-6. PEGylation of GSnP-6 at the side chain of the N-terminal Lys gives P-G6.

based assay more effectively than L- and P-selectin. Neutrophil adhesion to vascular endothelium is mediated by E-selectin and is a driver of acute vaso-occlusive crisis (VOC) in sickle cell disease. P-selectin is also upregulated on endothelial cells and both it and E-selectin bind adhesion molecules on red blood cells surfaces. Rivipansel was phase-III trialled in human patients with sickle cell disease (SCD) who were hospitalized for VOC and required treatment with intravenous opioids to reduce severe pain from having this condition. In a full analysis the median time to readiness for discharge (primary end point) was not different comparing treatment with Rivipansel and placebo and thus regulatory approval was not granted. However, a later statistical analysis (*post hoc*) showed early Rivipansel treatment within 26.4 hours of VOC pain onset had reduced median time to readiness for discharge by 41.5 hours, and reduced median time to discontinuation of IV opioids by 50.5 hours, compared with placebo (all $P < 0.05$), indicating that timing of Rivipansel administration after pain onset may be critical to achieving accelerated resolution of acute VOC in sickle cell disease patients.[69] More data was presented from the clinical study to support the proposal that Rivipansel targets E-selectin in patients, and it seems clear that the sulfate groups of Rivipansel do not interact optimally with P-selectin, compared to PSGL-1.

Uproleselan is another sLe[X] mimetic, modified with a polyethylene glycol (PEG) fragment. Although Uproleselan is not orally available, its pharmacokinetics and pharmacodynamics are much improved by the PEG residue. A phase 1/2 clinical study has recently completed where Uproleselan was added to chemotherapy in patients with relapsed or refractory acute myeloid leukemia (AML). The preliminary clinical study with Uproleselan reported promising initial outcomes such as a reduction in mucositis, a debilitating side effect of chemotherapy,[70] but, GlycoMimetics, Inc. recently reported that the primary endpoint was not attained.

3.5 Glycosulfopeptide mimetics for P-selectin

Chaikof and co-workers have rationally designed a more optimal PSGL-1 mimetic, GSnP-6, as a synthetic high-affinity

specific P-selectin ligand for human therapy (K_d = 22 nM).[71] The hydrolytically unstable tyrosine OSO_3^- groups of PSGL-1 are replaced with chemically stable $CH_2SO_3^-$ groups in GSnP-6; these modifications yield ~ 3 fold improved affinity for P-selectin, as compared to that for PSGL-1. Introduction of OSO_3^- groups by chemoenzymatic synthesis is also problematic due to stability issues with 3′-phosphoadenosine 5′-phosphosulfate, the required source of sulfate for all eukaryotic sulfations, providing another advantage of using the $CH_2SO_3^-$ modification in the peptide.

MD simulations were used to predict the stability of GSnP-6 bound to a P-selectin model and the structure of the calculated complex was comparable, only under conditions where His114 was fully protonated, to that of the crystal structure of P-selectin bound to PSGL-1, retaining all key non-covalent interactions. GSnP-6 also bound to E- and L-selectin (low μM range) albeit with lower affinity than for P-selectin.

PEGylation of GSnP-6 gave P-G6 (Fig. 5), which led to substantial increase in terminal half-life in plasma from several minutes for non-PEGylated structures to 15.65 ± 3.55 hours for P-G6, a very important development, giving a candidate with plasma half-life in the range of orally used anticoagulants. In preclinical study P-G6 inhibited P-selectin binding to murine and human leukocytes in a dose-dependent manner and reduced platelet–leukocyte aggregation *in vitro* and *in vivo*. P-G6 inhibited venous thrombosis in a preclinical model without impairing haemostasis.[72] Chaikof and co-workers described recently the gram scale synthesis GSnP-6 with a view to scale up synthesis for preclinical evaluation; they also show GSnP-6 displays dose-dependent inhibition of venous thrombosis *in vivo* and inhibits vaso-occlusive like events on a microvasculature-on-a-chip model system.[73]

3.6 Glycomimetics for siglecs

Sialic acid binding immunoglobulin-like lectins (siglecs) are immune cell lectins, found on the surfaces of most immune cells and are cell biomarkers.[74] Restricted expression patterns of siglecs have enabled therapies, such as an FDA antibody–drug conjugate, to be targeted to defined cell populations.[75] Liposomes decorated with siglec-1 ligands have been used to target antigen to macrophages.[76] Siglec-2 (CD-22), restricted to B-cells, is an endocytic receptor that is internalized and recycled to the cell surface.[77] Thus, siglecs have clear potential for selective delivery of drugs or other cargo to immune cells.[78] Siglecs are also targets for therapeutic intervention[79] as they inhibit immune cell activation and are associated with inflammatory diseases. Multivalency enhances ligand avidity for siglecs,[80] but, is associated with agonism of function, not antagonism. Features typical in binding of siglecs to sialic acid derivatives are evident in the crystal structure of mouse sialoadhesin (siglec 1) bonded to NeuAcα2-3Galβ1-4Glc (3′SL, 3′-sialyllactose), which discloses that most contacts are with the NeuAc residue (Fig. S3, ESI†).[81] NeuAc's carboxylate is coplanar with the guanidino group of Arg-97, a residue conserved across siglecs, and engaged in charged-charged H-bonding interactions.

The interaction of α-NeuAc is critical to recognition of mouse siglec-1 as the corresponding NeuAcβ-OMe failed to
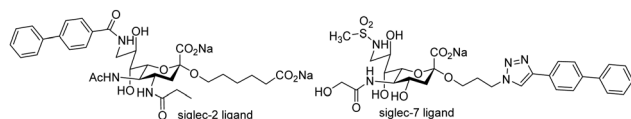
This journal is © The Royal Society of Chemistry 2024

Chem. Soc. Rev., 2024, **53**, 9428–9445 | **9435**

Fig. 6 Siglec-2 and siglec-7 glycomimetic ligands developed by Brossman and co-workers.

show evidence of binding by NMR study,[82] which is explained by the carboxyl group in NeuAcβ-OMe losing the interaction with the conserved Arg. Other interactions that occur are that the acetamide methyl group has contact with the indole ring of Trp, and the terminal carbon of the glycerol side chain (C9) is close to the indole of another Trp residue. The 9-OH establishes important H-bonding with the amide NH and carbonyl of a Leu residue of the siglec, while the amide nitrogen of the N-acetyl group forms a hydrogen bond with the main chain carbonyl of an Arg; these H-bond interactions are with residues in a β-strand peptide conserved among siglecs and likely sustained in glycomimetics (Fig. S3, ESI†).

Small molecule monomeric inhibitors of siglec-2, siglec-7[83,84] have been designed and synthesised. Identification of monomeric glycomimetic inhibitors of siglecs is considered highly important including comparison of their biological effects with multivalent ligands or antibodies. The compounds shown in Fig. 6 show significant enhancements in affinity for siglec-2/7 compared to NeuAc, the latter being conserved in siglec ligands.

Siglec-8, is an eosinophil- and mast-cell associated cell-surface receptor and is a target for the treatment of asthma. Siglec-8 has a role in accumulation and delayed apoptosis of activated eosinophils in the airways and a cause of persistent inflammation and tissue damage. Glycan microarray analyses[85] have revealed that the 6′-sulfo-sLe^X was selective for siglec-8 and structural information was generated by NMR[86] and more recently by X-ray crystallography (3.3 Å resolution).[87] Ernst and co-workers have successfully developed a higher affinity glycomimetic shown in Fig. 7,[88] which has a sulfonamide substituent in the 9-position and the polar Gal is replaced with a reduced polar carbocyclic scaffold to present the required sulfate. Compared to the 6′-sulfo-sLe^X, the affinity was improved ~20-fold. An induced fit binding mode where a hydrophobic pocket is created in siglec-8 to accommodate the naphthyl group is supported by the crystal structure. That monomeric inhibitors antagonise siglec-8 function, in contrast to multivalent ligands was recently demonstrated,[89] giving evidence of the importance to develop potent monomeric ligands as antagonists of siglecs.
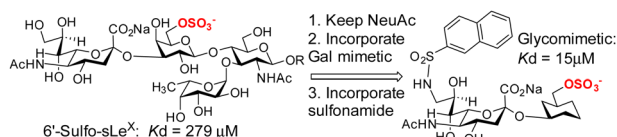
4. Multivalent ligand–lectin interactions

4.1 Mechanisms for avidity gain

Strong interactions are needed to promote adhesion between cells/particles or induce and sustain signal transduction and one mechanism by which this is achieved is via multivalency. Multivalent ligands are collections of small lectin ligands displayed on a scaffold and they tend to show enhancement in affinity compared to monomeric ligand, on a per mole of ligand basis,[90] which is termed the "glycoside cluster effect."[91] Investigations by Lee et al. using the asialoglycoprotein receptor (ASGPR) showed the distance between ligands (Gal or GalNAc) had to be enough (~20 Å) to enable simultaneous interaction with the trivalent ASGPR CRDs so that chelate type binding could arise (Fig. 8(B)). If spacing between the ligands and the CRDs are complimentary then large affinity gains are observed due to simultaneous binding of ligands.

There are various dissociation constants (K_d) for multivalent interaction. The K_{d3} (Fig. 8(B)) for the simultaneous binding interaction is the avidity.[92] The K_{d3} is lower than K_{d1} when the glycoside cluster effect (chelate binding) occurs. The K_{d1} is not a true measure of a single ligand–single lectin interaction as K_{d1} is also an avidity constant as the ligand and lectin are multivalent. The K_{d1} avidity arises due to statistical rebinding or the bind and jump mechanism (Fig. 8) when simultaneous binding of two ligands to two CRDs is not possible and is due to an increase in the on rate (k_{on}) relative to off rate (k_{off}) due to increased local ligand/lectin concentration because of multivalency.[93] The true single ligand single lectin interaction

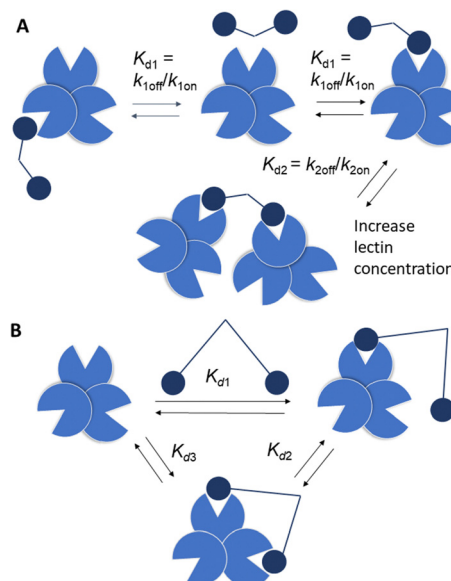Fig. 7 Evolution of a glycomimetic inhibitor for siglec-8.

Fig. 8 (A) Bind and jump mechanism (statistical rebinding). K_{d1} decreases for a bivalent ligand compared to a monomer due to increase of k_{on} relative to k_{off}. $K_{d2} > K_{d1}$ as number of available ligand binding sites is reduced and there may be increased steric interactions, reducing k_{on}. (B) Simultaneous binding to two CRDs is reflected by K_{d3} with $K_{d3} < K_{d1}$.

9436 | Chem. Soc. Rev., 2024, 53, 9428–9445
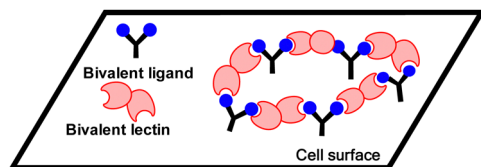
This journal is © The Royal Society of Chemistry 2024

Fig. 9 Crosslinking by bivalent ligands and bivalent lectins at a cell surface.

K_d, *i.e.* the affinity, would require the ligand and lectin to be monomeric.

A third mechanism involves crosslinking promoted by multivalent ligands and multivalent lectins that leads to aggregation, driving formation of a precipitate, which can complicate the picture given in Fig. 11.[94] Cross-linking can take place in the presence of a soluble lectin or at a cell surface and provides the basis for classical hemagglutination assays. At cell surfaces, cross-linking (Fig. 9) leads to receptor clustering, which leads to stronger and more prolonged signal transduction. Structure of crosslinked aggregates has biological relevance and was found, to influence galectin-1 mediated apoptosis.[95] The crosslinking with galectins, for example, can explain their role in bringing ligands to cell surfaces, such as occurs for tandem repeat type galectins (*e.g.* Gal4/8) and their interaction with sulfatide at cell surfaces (see Fig. 1).

4.2 Statistical rebinding glycocluster for modular vaccine design

The macrophage galactose C-type lectin (MGL) is a receptor on antigen presenting cells (APCs) that shows preferential binding for GalNAc. MGL is a trimeric C-type lectin receptor with distances estimated at ~ 82 Å between its CRDs, ~ 4-fold longer, than between the CRDs in its related trimer, ASGPR.[96] The tumour associated Tn antigen (GalNAcα1-O-Ser/Thr) is a ligand for MGL. The folding of MGL CRD and binding of GalNAc is Ca^{2+} ion dependant and involves chelation to the ion *via* its 3- and 4-OH groups. This coordination likely involves charge transfer to the Ca^{2+} ion enhancing the ligand CH polarization and strength of CH–π interaction, which has an electrostatic component.[97] The GalNAc–MGL binding[98] also includes CH–Pi interaction of 4-, 5- and 6-CH groups with the indole of Trp 271 (Fig. S5, ESI†). The *N*-acetyl group engages in CH–Pi interaction with the indole of Tyr-236 as well as carbonyl H-bonding with the amino group of Lys-264 and His-286's imidazole, explaining the ~ 70-fold

increase in affinity of GalNAc relative to Gal for hMGL.[99] The K_d measured for Gal by ITC was 210 μM.[100] The binding of GalNAc as determined by ITC is enthalpy driven ($K_d = 17.7$ μM, $-\Delta H = +47.2$ kJ mol^{-1}, $T\Delta S = -20.11$ kJ mol^{-1}).[101] As it has higher affinity than Gal, GalNAc was chosen as the monomeric ligand for multivalent ligand design to target MGL. Inhibition by a tetrameric tetraphenylethene (TPE) based glycocluster, which displays GalNAc, of binding of MGL to a surface neoglycoprotein presenting GalNAc by ELISA showed a remarkable $\sim 125\,000$-fold increase when compared to free GalNAc.[102] The bind and jump mechanism appears to contribute to enhancement of avidity for MGL as the distances between GalNAc residues in the TPE glycocluster are not sufficient to accommodate simultaneous binding. The TPE glycocluster did not inhibit a lectin specific for GlcNAc, and showed only low cross reactivity for galectins; it was shown to block MGL adherence to tissue sections.[103] Recently, a tripartite vaccine candidate (Fig. 10), which incorporated a trimeric version of the TPE glycocluster, conjugated to a tumour glycopeptide antigen and T-helper epitope showed greater uptake into DCs due to its avidity for MGL; the novel vaccine prototype also showed enhanced humoral response, demonstrating the potential for highly avid glycoclusters targeting MGL on immune cells for vaccine research. The tumour antigen segment of the prototype, by itself, has good avidity for MGL as it already presents GalNAc residues on the glycopeptide. However, when the trimeric TPE glycocluster was conjugated there was ~ 10-fold further avidity improvement.[104]

4.3 Simultaneous binding of glycoclusters to block influenza

The influenza virus hemagglutinin (HA) is a homotrimeric surface lectin that interacts with NeuAc containing ligands. NeuAc shows a network of electrostatic interactions, including H-bonding and indole–CH$_3$ contact (Fig. S3, ESI†).[105] Research on developing small molecule ligands for HA based on NeuAc, has, thus far, not yielded very potent inhibitors. A serendipitously identified HA ligand, *N*-cyclohexyltaurine, was found to mimic interactions of broadly neutralizing antibodies and that of NeuAc, which might offer potential to identify low molecular weight ligands with no carbohydrate character.[106]

Recognition by HA of host cell glycans has been associated with human type influenza specificity for the NeuAcα-2,6-Gal compared to NeuAcα2,3-Gal, the latter being associated with avian influenza.[107] Higher avidity is observed in the recognition of biantennary *N*-glycans, containing NeuAcα2,6GalNAc of the
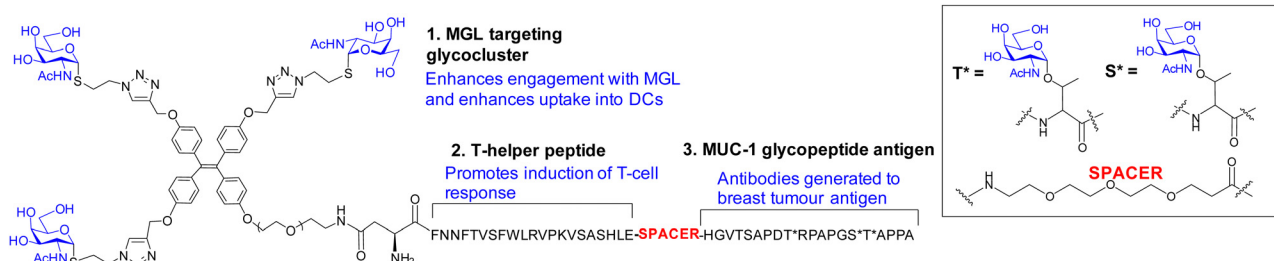

Fig. 10 Modular vaccine design using TPE glycocluster to engage MGL at APC surface.

human airway by HA compared to those based on NeuAcα2,3-GalNAc. The K_d for NeuAcα2,3GalNAc shows only ∼1.5-fold lower potency than the 2,6-disaccharide (3.1 ± 0.4 mM $vs.$ 2.0 ± 0.2 mM) for binding to the HA of the H3N2 viral strain A/HongKong/1/1968.[108] The NeuAcα2,6Gal canonical specificity is explained by extensive presentation of this disaccharide on glycans of epithelial cells of the human airway, where multivalency leads to increase selectivity for NeuAcα-2,6Gal.[109] Recent work has provided insight into the origin of an evolved specificity increase for a subtype of biantennary N-glycans.[110] Specifically, two NeuAcα2,6Gal residues are projected in an optimal geometry for simultaneous binding to two CRDs in the HA trimer; the HA ligand binding sites are spaced about 45 Å apart in the HA trimer and the chelate binding accounts for >100-fold enhancement of avidity as measured by ELISA. This avidity and specificity gain has been maintained by influenza virus HA variants for biantennary N-glycans containing multiple LacNAc repeat units found in airway tissue glycomes. The high avidity associated with chelate type binding to bivalent N-glycans is due to NeuAcα2,6Gal being located at the end of chains having 3/4 LacNAc spacer groups. The spacing between NeuAc residues for simultaneous binding is not accessible either for N-glycans presenting NeuAcα2,3Gal with 3/4 LacNAc spacer groups or N-glycans presenting NeuAcα2,6Gal with only 1 or 2 spacer LacNAcs because the latter cannot simultaneously bind to two CRDs (Fig. 11). Influenza virus has caused several pandemics[111] and the development of infection blockers is of interest. Such insights from how native glycans interact are, thus, enabling design and synthesis of glycocluster ligands designed with the appropriate spacing to enable simultaneous binding to at least two of HA's CRDs.[112] Pieters and co-workers prepared the dimeric NeuAc presenting glycocluster in Fig. 12 that showed an IC$_{50}$ of 0.7 μM, representing a 428-fold enhancement over the reference ligand. Thus, precisely designed multivalent ligands may address need to develop influenza infection blockers.
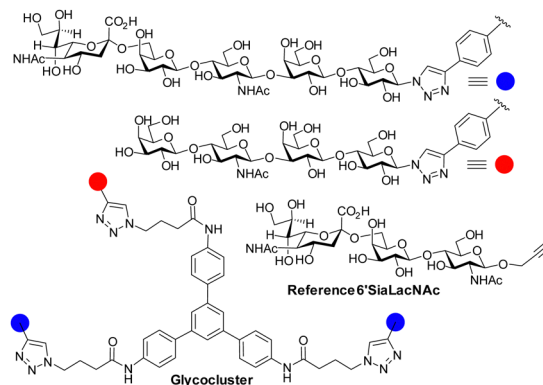

Fig. 12 HA ligands for structure activity relationships, including chelating ligands.

4.4 Avidity boosting by combining statistical rebinding with simultaneous binding for langerin and DCSIGN

Recent attempts have been made to combine statistical rebinding with simultaneous binding to boost avidity of multivalent ligands. Seitz and co-workers produced DNA–peptide nucleic acid (PNA) complexes as scaffolds to precisely display two glycoclusters, to probe the impact of distance on binding to langerin, a trimeric cell surface lectin with three CRDs located at ∼42 Å distances apart.[113] The DNA–PNA complexes form by Watson–Crick hybridization of 39 nucleotide long DNA template strands in the presence of three complimentary 13 nt peptide nucleic acid (PNA) strands. A selection of the construct is shown in Fig. 13, based on the langerin ligand GlcNHTs. The distances between the trimeric glycoclusters varied from ∼16 Å to 104 Å.

The trimeric glycocluster presenting GlcNHTs shows avidity increase compared to GlcNHTs of ∼7-fold. The presentation of the GlcNHTs ligand as a monomer on the PNA–DNA hybrid showed an increase of ∼3-fold over GlcNHTs, while presentation of one trimeric glycocluster on PNA–DNA showed ∼10-fold avidity

Fig. 11 Affinity/avidity for selected glycans for influenza virus HA. Weak binding is observed for single ligands and for bivalent ligands where the spacing between NeuAc residues does not facilitate simultaneous ligand binding. Strong binding is observed for biantennary extended N-glycans with 3/4 LN spacer groups like 6SLN$_4$-N, but not 3SLN$_4$-N.

9438 | Chem. Soc. Rev., 2024, 53, 9428–9445

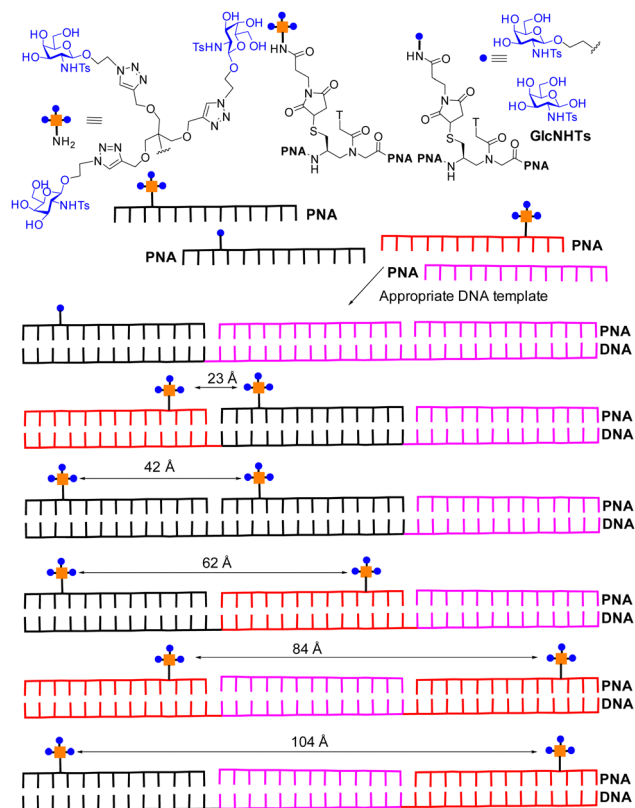This journal is © The Royal Society of Chemistry 2024

Fig. 13 DNA–PNA hybrids for targeting langerin. Strongest binding is observed for hexavalent compound where two trimeric glycoclusters are separated by distances of 42 Å, matching the distance of 42 Å between CRDs in langerin.
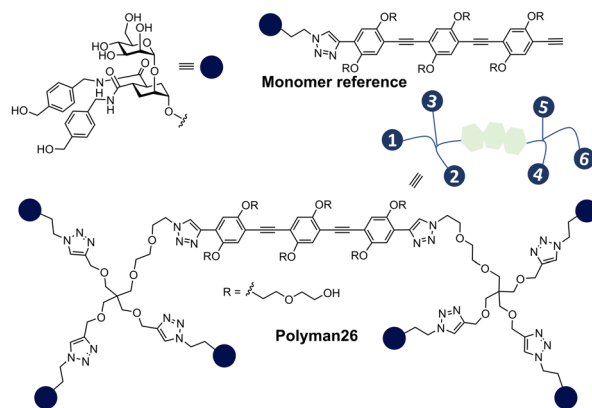

Fig. 14 DC-SIGN ligands: monomer reference ligand and polyman26.

updated using a surface that preserves the tetrameric form of DC-SIGN, accessibility to its CRDs and their topology and thus appropriate to dissect the contribution of statistical rebinding and chelate binding from ligands. Polyman26 had an apparent K_d = 11.5 ± 2.3 nM and was 570-fold more potent per mole of ligand than the reference compound (K_d = 39 300 ± 3900 nM).[116] MD simulations predicted that simultaneous binding of two headgroups from polyman26 was feasible to two DC-SIGN CRDs, contributing most to the observed avidity increase, boosted in turn by statistical rebinding. The chelate binding was facilitated by flexibility in the DC-SIGN structure allowing movement of the CRDs and induced fitting (Fig. 15).

4.5 Promotion or prevention of receptor cross-linking in multivalent ligand design

Reymond and co-workers designed galactopyranoside based glycoclusters that were both chelating ligands for the LecA lectin of the *Pseudomonas aeruginosa* (PA) pathogen leading to high avidity gain, but which could also show the ability to promote aggregation. The combining of simultaneous binding of ligands to two LecA sites and crosslinking led to more effective biofilm inhibitors.[117]

The formation of precipitates *via* crosslinking is associated with plaque formations and there are instances where it is not desired from a biomedical viewpoint. Wittman and co-workers synthesised compounds with high avidity for WGA, based on ligands that show simultaneous binding to four GlcNAc binding sites in a WGA dimer. The ligands had K_d values in the low nM range. One inline tetravalent ligand (Fig. 16) showed one to

enhancement over the monomer on the PNA–DNA hybrid. Spacing of two trimeric glycoclusters at ∼23 Å on PNA–DNA gave a further enhancement of ∼13-fold; the distances between the trimeric glycocluster is substantially less than 42 Å and not sufficient to facilitate simultaneous binding to two langerin CRDs and the avidity gain is thus explained by statistical rebinding only (bind and jump). A hybrid with ∼42 Å distance between the glycoclusters, matching that between langerin CRDs, showed the highest avidity, which is explained to be due to the combination of statistical rebinding combined with chelate binding. Subsequent cell binding studies indicated the more potent hybrids could also bind to Langerhan cell surfaces, which express langerin. Ligands with high avidity for langerin have potential for targeting vaccines to Langerhans cells for improved therapeutic effect.

Bernardi, Fieschi and co-workers had earlier aimed to take advantage of both chelation and statistical rebinding in the modular design of ligands for DC-SIGN, which have two trivalent glycoclusters presented on a rigid core of defined length.[114] DC-SIGN is a homotetrameric lectin with four CRDs at the C-terminus of each monomer in a square-like arrangement; the distance between the CRDs in DC-SIGN is ∼39 Å (width) and ∼52 Å (length) and ∼60 Å (across the diagonal), assuming the CRDs are at the corners of a rectangle.[115] They synthesised the divalent binder construct, polyman26, with nanomolar range affinity (Fig. 14). The evaluation of polyman26 was recently

Fig. 15 Cooperation of statistical rebinding and simultaneous binding.

This journal is © The Royal Society of Chemistry 2024

Chem. Soc. Rev., 2024, **53**, 9428–9445 | 9439

Fig. 16 Multivalent lectin ligands with inline topology (iLecs) bind simultaneously to four GlcNAc binding sites in WGA leading to high avidity with no precipitation.

two million-fold avidity increase per GlcNAc residue. Various evidence, including EPR using spin labelled inline ligands, supported simultaneous binding of the four GlcNAc to the four WGA binding sites. There was no evidence for crosslinking of the inline tetravalent ligand, *i.e.* no precipitation was observed. Crosslinking was observed for ligands with shorter distances between the GlcNAcs when simultaneous binding is not possible.[118]

4.6 Glycoclusters for LYTACs, cell targeting of antisense nucleotides and for diagnostics

Targeted protein degradation has emerged as a strategy for therapeutic development and as a tool for chemical biology, with proteolysis targeting chimeras (PROTACs) gaining most attention thus far.[119] Bertozzi's group developed lysosome targeting chimeras (LYTACs) by conjugating a polyvalent ligand, based on Man-6-phosphate, to a small molecule or antibody that binds a protein to be degraded; the pol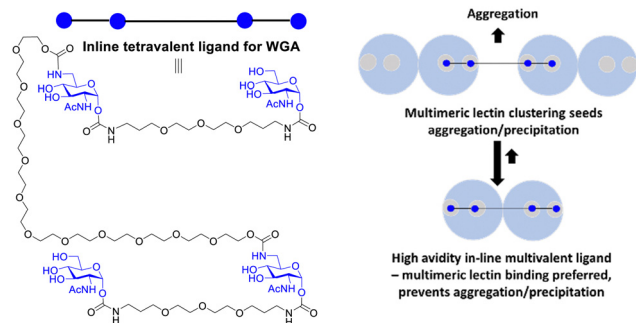yvalent ligand targets the cation-independent mannose-6-phosphate receptor (CI-M6PR),[120] triggering internalization of the desired target through CI-M6PR mediated endocytosis, leading to transport to the lysosome and protein degradation. Lectin ASGPR is another lysosomal targeting receptor, with ASGPR responsible for clearing glycoproteins *via* endocytosis and lysosomal degradation, particularly in liver cells. Hence, Zhou *et al.* used high avidity ASGPR glycocluster ligands in LYTACs.[121] In another development, ASGPR targeting glycoclusters increase the delivery of antisense nucleotides to hepatocytes enabling development of therapies for what had been considered undruggable protein targets.[122,123] Givosiran is a small interfering ribonucleic acid (siRNA) that is conjugated to a trivalent GalNAc glycocluster to enhance the delivery and effectiveness of siRNA.[124] Givosiran, obtained regulatory approval from the FDA for treatment of acute hepatic porphyria in 2019.[125] Other siRNA–GalNAc glycocluster conjugates are in advanced clinical studies or approved[126] (lumirsiran, inclisiran, eplontersen). Another application developed for GalNAc glycocluster ligands is in synthesis of positron emission tomography (PET) diagnostic probes to measure ASGPR expression, reduced in nonalcoholic steatohepatitis, where early diagnosis may enable prevention of life-threatening diseases associated with this condition.[127] In one other recent development, a luminescent glycocluster molecular sensor system, which showed reliable enhancement of lanthanide ion centred emission in the presence of unlabelled lectins have been developed. This work by Byrne and co-workers included sensing of the bacterial lectin LecA, which is lectin of the priority ESCAPE pathogen PA.[128]

5. Conclusions and perspectives

Lectin–ligand interactions mediate important biological processes and research is leading to new clinically studied inhibitors, prototype vaccines, targeting agents for delivery, diagnostics and tools for chemical biology based on small monomeric ligand or glycocluster development.

Glycans have well-defined 3D structural preferences and the conformation of the free ligand is often very similar to that bound by the lectin. The availability of structural information is enabling improved ligand design. There are relatively few X-ray crystal structures of oligosaccharides in the Cambridge Crystallographic Datacentre, although information is often accessible from co-crystal structural coordinates deposited at the Protein Data Bank. Moreover, computational tools are being developed and made openly available to non-specialists for generating low-energy conformers for glycans which can be used in new ligand design.[129] The recent development of cryo-electron microscopy has the potential to give atomic-level detail of the interaction of glycoproteins/glycoclusters with lectins and reveal new strategies for ligand design,[130] especially where there is very limited experimentally derived information, such as for structures of multivalent ligands bound to multimeric lectins, with reliance in many cases on computing simulations, including AI based alphafold[131] to give potential geometries.[132]

Native glycan ligands do not have ideal properties as pharmaceuticals. However, glycans are inspiring the development of drug-like glycomimetics. The use of synthetic chemistry for producing such substances, is essential. Factors determining lectin–ligand binding affinities are complex, determined by type and strength of interaction, binding pocket shape and solvent effects. Glycomimetic design includes substituting part of natural ligand with other functional groups or scaffolds to (i) enhance affinity or selectivity/specificity for a target lectin; (ii) increase stability *in vitro* and *in vivo* such as with use of *S*-glycosides; (iii) increase other physicochemical and pharmacokinetic properties such as by reducing polar surface area of ligand to enhance oral availability or (iv) appending PEG groups to increase half-time in plasma. Binding free energies have been improved by strategies which include conformational preorganisation of binding groups. Ernst's group have shown that binding free energies can be more favourable after replacing part of the glycan which has a purely structural role by a more hydrophobic scaffold with reduced polarity. As typified for galectin-3 ligand development led by Nilsson, Leffler and co-workers the generation of new interactions contribute to affinity enhancement. Areas where monomeric ligand inhibitors continue to be investigated include for galectins, for siglecs as

9440 | *Chem. Soc. Rev.*, 2024, **53**, 9428–9445

This journal is © The Royal Society of Chemistry 2024

well as for lectins involved in anti-microbial resistance such as FimH,[133] LecA[134] and LecB.[135]

Conjugating multiple small lectin ligands to scaffolds to give multivalent ligands is a well-developed strategy to improve avidity and selectivity. There is now proven clinical success in use of multivalent ligands as a component of new siRNA medicines for delivery purposes which leads to enhanced uptake and efficacy,[136] which is a milestone for the field. There is potential for expansion of this approach to other lectins and cell types. Multivalent ligands act as delivery agents and agonists for siglecs, in contrast to monomeric ligands, which act as antagonists, showing the need to optimise both monomeric and multivalent ligands, which will depend on the desired application.

Avidities of multivalent ligands are influenced by geometrical factors such as spacing between individual ligands and whether they can match the distances between CRDs. Higher avidity is observed for glycoclusters where chelate binding is enabled by matching spacing between ligands and CRDs. It has been shown that further benefits arise from combining statistical rebinding with chelate binding as seen more recently for DCSIGN and langerin. Developing chelate binding ligands is likely more challenging for a lectin like MGL where distances between CRDs are $\sim$80 Å, in contrast with distances $\sim$20–25 Å for ASGPR but developing approaches to targeting such CRDs with chelate binding ligands over large distances could be important. Despite the distance requirement for MGL potent glycocluster ligands have emerged based on a tetraphenylethene (TPE) scaffold, which can deliver glycopeptide tumour vaccines via MGL targeting and the resulting improved humoral response has been shown in vivo. How TPE ligands work effectively is not clear; reversible formation of small aggregates of TPE glycocluster in water that engage in chelate binding seems possible and could be contributing to improved avidity. The investigation of aggregating scaffolds could be a strategy to further explore for multivalent ligand design either with TPE or related aggregating scaffolds. It would also be interesting to evaluate aggregating glycoclusters for other lectins. Another multivalent ligand mechanism which is relevant for soluble lectins is cross-linking. Research from Wittman's group shows how precipitation, via crosslinking can be avoided by careful design of very potent inline multivalent ligands based on simultaneous binding with optimised geometries. On the other hand increasing the cross-linking efficiency was shown to be useful for developing biofilm inhibitors, which is important in antimicrobial research.

There are many opportunities as development of ligands for lectins is still at a relatively early stage, and potent ligands with desirable properties are still lacking for many lectin targets. It is expected that development of new ligands for application in glycoscience and glycomedicine will be a very active research area for the foreseeable future.

Author contributions

PVM sourced and analysed data, planned, wrote, and revised the manuscript. AD, SK, LF, EH, and KM sourced data and contributed to drafting and/or editing.

Data availability statement

The data supporting this tutorial review have been included with the ESI† or are found in the cited references.

Conflicts of interest

There are no conflicts to declare.

Acknowledgements

Notes and references

1 A. Varki and S. Kornfeld Historical, Background and Overview, in *Essentials of Glycobiology*, ed. A. Varki, R. D. Cummings, J. D. Esko, P. Stanley, G. W. Hart, M. Aebi, D. Mohnen, T. Kinoshita, N. H. Packer, J. H. Prestegard, R. L. Schnaar and P. H. Seeberger, Cold Spring Harbor Laboratory Press, Cold Spring Harbor, 4th edn, 2022. ch. 1.

2 M. E. Taylor, K. Drickamer, A. Imberty, Y. van Kooyk, R. L. Schnaar, M. E. Etzler and A. Varki, Discovery and Classification of Glycan-Binding Proteins, in *Essentials of Glycobiology*, ed. A. Varki, R. D. Cummings, J. D. Esko, P. Stanley, G. W. Hart, M. Aebi, D. Mohnen, T. Kinoshita, N. H. Packer, J. H. Prestegard, R. L. Schnaar, P. H. Seeberger, Cold Spring Harbor Laboratory Press, Cold Spring Harbor (NY), 4th edn, 2022, ch. 28.

3 (a) N. Jayaraman, *Chem. Soc. Rev.*, 2009, **38**, 3463–3483; (b) R. Roy, P. V. Murphy and H. J. Gabius, *Molecules*, 2016, **21**, 629.

4 H. J. Gabius, M. Cudic, T. Diercks, H. Kaltner, J. Kopitz, K. H. Mayo, P. V. Murphy, S. Oscarson, R. Roy, A. Schedlbauer, S. Toegel and A. Romero, *ChemBioChem*, 2022, **23**, e2021003.

5 V. S. R. Rao, P. K. Qasba, P. V. Balaji and R. Chandrasekaran, *Conformation of Carbohydrates*, Harwood Academic Publishers, 1998, pp. 309.

6 V. S. R. Rao, P. K. Qasba, P. V. Balaji and R. Chandrasekaran, *Conformation of Carbohydrates*, Harwood Academic Publishers, 1998, pp. 49–190.

7 A. Y. Mehta and R. D. Cummings, *Bioinformatics*, 2020, **36**, 3613–3614.

8 (a) J. T. Edward, *J. Chem. Ind.*, 1955, 1102–1104; (b) R. U. Lemieux, Rearrangements and Isomerizations in Carbohydrate Chemistry, in *Molecular Rearrangements*, ed. P. De Mayo, Interscience, New York, 1964, pp. 709–769.

This journal is © The Royal Society of Chemistry 2024

Chem. Soc. Rev., 2024, **53**, 9428–9445 | **9441**

9 I. V. Alabugin, L. Kuhn, N. V. Krivoshchapov, P. Mehaffy and M. G. Medvedev, *Chem. Soc. Rev.*, 2021, **50**, 10212–10252.

10 K. B. Wiberg, W. F. Bailey, K. M. Lambert and Z. Stempel, *J. Org. Chem.*, 2018, **83**, 5242–5255.

11 L. Kerins, S. Byrne, A. Gabba and P. V. Murphy, *J. Org. Chem.*, 2018, **83**, 7714–7729.

12 For ethane-1,2-diol there is an increased preference for the *gauche* arrangement of the electron withdrawing oxygen atoms, sometimes attributed to intramolecular H-bonding. For 1,2-dimethoxyethane, where there is no H-bonding, there is still an increase in preference for the *gauche* arrangement. The *gauche* effect is stronger for fluorinated derivatives. See (*a*) S. Wolf, *Acc. Chem. Res.*, 1970, **5**, 102–111; (*b*) M. Andersson and G. Karlstrom, *J. Phys. Chem.*, 1985, **89**, 4957–4962.

13 Y. Yu and M. Delbianco, *Chem. – Eur. J.*, 2020, **26**, 9814.

14 A. J. Petrescu, S. M. Petrescu, R. A. Dwek and M. R. Wormald, *Glycobiology*, 1999, **9**, 343–352.

15 Woods Group. (2005-XXXX) GLYCAM Web. Complex Carbohydrate Research Center, University of Georgia, Athens, GA. (https://legacy.glycam.org).

16 (*a*) S. Kumar, M. Frank and R. Schwartz-Albiez, *PLoS One*, 2013, **8**, e59761; (*b*) V. Palivec, C. Johannessen, J. Kaminsky and H. Martinez-Seara, *PLoS Comput. Biol.*, 2022, **18**, e1009678; (*c*) P. Vidal, J. Jiménez-Barbero and J. F. Espinosa, *Carbohydr. Res.*, 2016, **433**, 36–40; (*d*) S. Sabesan, K. Bock and J. C. Paulson, *Carbohydr. Res.*, 1991, **218**, 27–54.

17 M. Martín-Pastor, A. Canales, F. Corzana, J. L. Asensio and J. Jiménez-Barbero, *J. Am. Chem. Soc.*, 2005, **127**, 3589–3595.

18 (*a*) K. Hirotsu and A. Shimada, *Bull. Chem. Soc. Jpn.*, 1974, **47**, 1872–1879; (*b*) Coordinates are available Cambridge Crystallographic Data Centre. https://www.ccdc.cam.ac.uk/CSDentry=BLACTO.

19 U. Olsson, E. Sawen, R. Stenutz and G. Widmalm, *Chem. – Eur. J.*, 2009, **15**, 8886–8894.

20 C. W. von der Lieth, H. C. Siebert, T. Kožár, M. Burchert, M. Frank, M. Gilleron, H. Kaltner, G. Kayser, E. Tajkhorshid, N. V. Bovin, J. F. G. Vliegenthart and H. J. Gabius, *Acta Anat.*, 1998, **161**, 91–109.

21 (*a*) E. W. Sayers and J. H. Prestegard, *Biophys. J.*, 2000, **79**, 3313–3329; (*b*) E. W. Sayers and J. H. Prestegard, *Biophys. J.*, 2002, **82**, 2683–2699.

22 T. Chandran, A. Sharma and M. Vijayan, *Adv. Protein Chem. Struct. Biol.*, 2013, **92**, 135–178.

23 M. M. Sauer, R. P. Jakob, J. Eras, S. Baday, D. Eriş, G. Navarra, S. Bernèche, B. Ernst, T. Maier and R. Glockshuber, *Nat. Commun.*, 2016, **7**, 10738.

24 E. V. Sokurenko, V. Vogel and W. E. Thomas, *Cell Host Microbe*, 2008, **4**, 314–323.

25 C. S. Hung, J. Bouckaert, D. Hung, J. Pinkner, C. Widberg, A. DeFusco, C. G. Auguste, R. Strouse, S. Langermann, G. Waksman and S. J. Hultgren, *Mol. Microbiol.*, 2002, **44**, 903–915.

26 A. Wellens, M. Lahmann, M. Touaibia, J. Vaucher, S. Oscarson, R. Roy, H. Remaut and J. Bouckaert, *Biochemistry*, 2012, **51**, 4790–4799.

27 M. M. Sauer, R. P. Jakob, T. Luber, F. Canonica, G. Navarra, B. Ernst, C. Unverzagt, T. Maier and R. Glockshuber, *J. Am. Chem. Soc.*, 2019, **141**, 936–944.

28 L. A. Lasky, *Annu. Rev. Biochem.*, 1995, **64**, 113–139.

29 W. S. Somers, J. Tang, G. D. Shaw and R. T. Camphausen, *Cell*, 2000, **103**, 467–479.

30 R. C. Preston, R. P. Jakob, F. P. Binder, C. P. Sager, B. Ernst and T. Maier, *J. Mol. Cell Biol.*, 2016, **8**, 62–72.

31 K. L. Hudson, G. J. Bartlett, R. C. Diehl, J. Agirre, T. Gallagher, L. L. Kiessling and D. N. Woolfson, *J. Am. Chem. Soc.*, 2015, **137**, 15152–15160.

32 E. P. Mitchell, C. Sabin, L. Šnajdrová, M. Pokorná, S. Perret, C. Gautier, C. Hofr, N. Gilboa-Garber, J. Koča, M. Wimmerová and A. Imberty, *Proteins*, 2005, **58**, 735–746.

33 P. V. Murphy, A. Romero, Q. Xiao, A. K. Ludwig, S. Jogula, N. V. Shilova, T. Singh, A. Gabba, B. Javed, D. Zhang, F. J. Medrano, H. Kaltner, J. Kopitz, N. V. Bovin, A. M. Wu, M. L. Klein, V. Percec and H. J. Gabius, *iScience*, 2021, **24**, 101919.

34 C. A. Fitch, D. A. Karp, K. K. Lee, W. E. Stites, E. E. Lattman and E. B. García-Moreno, *Biophys. J.*, 2002, **82**, 3289–3304.

35 C. P. Sager, D. Eriş, M. Smieško, R. Hevey and B. Ernst, *Beilstein J. Org. Chem.*, 2017, **13**, 2584–2595.

36 E. J. Toone, *Curr. Opin. Struct. Biol.*, 1994, **4**, 719–728.

37 D. Gupta, T. K. Dam, S. Oscarson and C. F. Brewer, *J. Biol. Chem.*, 1997, **272**, 6388–6392.

38 J. D. Chodera and D. L. Mobley, *Annu. Rev. Biophys.*, 2013, **42**, 121–142.

39 C. P. Sager, B. Fiege, P. Zihlmann, R. Vannam, S. Rabbani, R. P. Jakob, R. C. Preston, A. Zalewski, T. Maier, M. W. Peczuh and B. Ernst, *Chem. Sci.*, 2018, **9**, 646–654.

40 L. Pang, J. Bezençon, S. Kleeb, S. Rabbani, A. Sigl, M. Smiesko, C. P. Sager, D. Eris, O. Schwardt and B. Ernst, *Carbohdr. Chem.*, 2016, **42**, 248–273.

41 B. Ernst and J. L. Magnani, *Nat. Rev. Drug Discovery*, 2009, **8**, 661–677.

42 A. Tamburrini, C. Colombo and A. Bernardi, *Med. Res. Rev.*, 2020, **40**, 495–531.

43 U. Schmitz and S. Swaminathan, *Antiviral Ther.*, 2022, **27**, 13596535211067598.

44 R. D. Cummings, F. T. Liu, G. A. Rabinovich, S. R. Stowell and G. R. Vasta, Galectins, in *Essentials of Glycobiology*, ed. A. Varki, R. D. Cummings and J. D. Esko *et al.*, Cold Spring Harbor Laboratory Press, Cold Spring Harbor (NY), 4th edn, 2022, ch. 36.

45 K. V. Mariño, A. J. Cagnoni, D. O. Croci and G. A. Rabinovich, *Nat. Rev. Drug Discovery*, 2023, **22**, 295–316.

46 R. P. M. Dings, M. C. Miller, R. J. Griffin and K. H. Mayo, *Int. J. Mol. Sci.*, 2018, **19**, 905.

47 H. Ideo, A. Seko, I. Ishizuka and K. Yamashita, *Glycobiology*, 2003, **13**, 713–723.

48 H. Yoshida, S. Yamashita, M. Teraoka, A. Itoh, S. I. Nakakita, N. Nishi and S. Kamitori, *FEBS J.*, 2012, **279**, 3937–3951.

49 P. Sörme, P. Arnoux, B. Kahl-Knutsson, H. Leffler, J. M. Rini and U. J. Nilsson, *J. Am. Chem. Soc.*, 2005, **127**, 1737–1743.

9442 | *Chem. Soc. Rev.*, 2024, **53**, 9428–9445

This journal is © The Royal Society of Chemistry 2024

50 W. Schneider, *Ber. Dtsch. Chem. Ges.*, 1919, **52B**, 2135–2149.

51 H. Leffler and S. H. Barondes, *J. Biol. Chem.*, 1986, **261**, 10119–10126.

52 S. R. Stowell, Y. Qian, S. Karmakar, N. S. Koyama, M. Dias-Baruffi, H. Leffler, R. P. McEver and R. D. Cummings, *J. Immunol.*, 2008, **180**, 3091–3102.

53 A. MacKinnon, W. S. Chen, H. Leffler, N. Panjwani, H. Schambye, T. Sethi and U. J. Nilsson, *Top. Med. Chem.*, 2014, **12**, 95–121.

54 T. J. Hsieh, H. Y. Lin, Z. Tu, T. C. Lin, S. C. Wu, Y. Y. Tseng, F. T. Liu, S. T. D. Hsu and C. H. Lin, *Sci. Rep.*, 2016, **6**, 29457.

55 E. Montero, A. García-Herrero, J. L. Asensio, K. Hirai, S. Ogawa, F. Santoyo-González, F. J. Cañada and J. Jiménez-Barbero, *Eur. J. Org. Chem.*, 2000, 1945–1952.

56 A. Kumar, M. Paul, M. Panda, S. Jayaram, N. Kalidindi, H. Sale, M. Vetrichelvan, A. Gupta, A. Mathur, B. Beno, A. Regueiro-Ren, D. Cheng, M. Ramarao and K. Ghosh, *Glycobiology*, 2021, **31**, 1390–1400.

57 N. Hirani, A. C. MacKinnon, L. Nicol, P. Ford, H. Schambye, A. Pedersen, U. J. Nilsson, H. Leffler, T. Sethi, S. Tantawi, L. Gravelle, R. J. Slack, R. Mills, U. Karmakar, D. Humphries, F. Zetterberg, L. Keeling, L. Paul, P. L. Molyneaux, F. Li, W. Funston, I. A. Forrest, A. J. Simpson, M. A. Gibbons and T. M. Maher, *Eur. Respir. J.*, 2021, **57**, 2002559.

58 News release Aug. 15 2023. Downloaded 12/01/2024. https://ir.galecto.com/news-releases/news-release-details/galecto-announces-topline-results-phase-2b-galactic-1-trial.

59 F. R. Zetterberg, A. MacKinnon, T. Brimert, L. Gravelle, R. E. Johnsson, B. Kahl-Knutson, H. Leffler, U. J. Nilsson, A. Pedersen, K. Peterson, J. A. Roper, H. Schambye, R. J. Slack and S. Tantawi, *J. Med. Chem.*, 2022, **65**, 12626–12638.

60 T. Brimert, R. Johnsson, H. Leffler, U. Nilsson and F. Zetterberg, WO2016120403, 2016.

61 F. R. Zetterberg, K. Peterson, R. E. Johnsson, T. Brimert, M. Hakansson, D. T. Logan, H. Leffler and U. J. Nilsson, *ChemMedChem*, 2018, **13**, 133–137.

62 F. P. C. Binder, K. Lemme, R. C. Prestin and B. Ernst, *Angew. Chem., Int. Ed.*, 2012, **51**, 7327–7331.

63 W. S. Somers, J. Tang, G. D. Shaw and R. T. Camphausen, *Cell*, 2000, **103**, 467–479.

64 H. C. Kolb and B. Ernst, *Chem. – Eur. J.*, 1997, **3**, 1571.

65 A. J. Ruben, Y. Kiso and E. Freire, *Chem. Biol. Drug Design*, 2006, **67**, 2–4.

66 R. C. Preston, R. P. Jakob, F. P. C. Binder, C. P. Sager, B. Ernst and T. Maier, *J. Mol. Cell Biol.*, 2016, **8**, 62–72.

67 J. Egger, C. Weckerle, B. Cutting, O. Schwardt, S. Rabbani, K. Lemme and B. Ernst, *J. Am. Chem. Soc.*, 2013, **135**, 9820–9828.

68 (*a*) J. Chang, J. T. Patton, A. Sarkar, B. Ernst, J. L. Magnani and P. S. Frenette, *Blood*, 2010, **116**, 1779–1786; (*b*) J. L. Magnani, J. T. Patton, A. K. Sarkar, S. A. Svarovsky and B. Ernst, WO2007028050A1, 2007.

69 C. D. Dampier, M. J. Telen, T. Wun, R. Clark Brown, P. Desai, F. El Rassi, B. Fuh, J. Kanter, Y. Pastore, J. Rothman, J. G. Taylor, D. Readett, K. M. Sivamurthy, B. Tammara, L. J. Tseng, J. Nelson Lozier, H. Thackray, J. L. Magnani and K. L. Hassell, *Blood*, 2023, **141**, 168–179.

70 D. J. DeAngelo, B. A. Jonas, J. L. Liesveld, D. L. Bixby, A. S. Advani, P. Marlton, J. L. Magnani, H. M. Thackray, E. J. Feldman, M. E. O'Dwyer and P. S. Becker, *Blood*, 2022, **139**, 1135–1146.

71 V. Krishnamurthy, M. Sardar, Y. Ying, X. Song, C. Haller, E. Dai, X. Wang, D. Hanjaya-Putra, L. Sun, V. Morikis, S. I. Simon, R. J. Woods, R. D. Cummings and E. L. Chaikof, *Nat. Commun.*, 2015, **6**, 6387.

72 D. J. Wong, D. D. Park, S. S. Park, C. A. Haller, J. Chen, E. Dai, L. Liu, A. R. Mandhapati, P. Eradi, B. Dhakal, W. J. Wever, M. Hanes, L. Sun, R. D. Cummings and E. L. Chaikof, *Blood*, 2021, **138**, 1182–1193.

73 B. Dhakal, A. Mandhapati, P. Eradi, S. Park, K. Fibben, K. Li, A. DeYong, S. Escopy, G. Karki, D. D. Park, C. A. Haller, E. Dai, L. Sun, W. A. Lam and E. L. Chaikof, *J. Am. Chem. Soc.*, 2024, **146**, 17414–17427.

74 M. S. Macauley, P. R. Crocker and J. C. Paulson, *Nat. Rev. Immunol.*, 2014, **14**, 653.

75 C. Selby, L. R. Yacko and A. E. Glode, *J. Adv. Pract. Oncol.*, 2019, **10**, 68–82.

76 W. C. Chen, N. Kawasaki, C. M. Nycholat, S. Han, J. Pilotte, P. R. Crocker and J. C. Paulson, *PLoS One*, 2012, **7**, e39039.

77 M. K. O'Reilly, H. Tian and J. C. Paulson, *J. Immunol.*, 2011, **186**, 1554–1563.

78 (*a*) P. R. Crocker, J. C. Paulson and A. Varki, *Nat. Rev. Immunol.*, 2007, **7**, 255–266; (*b*) H. Läubli, K. Kawanishi, C. G. Vazhappilly, R. Matar, M. Merheb and S. S. Siddiqui, *FEBS J.*, 2021, **288**, 6206–6225.

79 B. A. H. Smith and C. R. Bertozzi, *Nat. Rev. Drug Discovery*, 2021, **20**, 217–243.

80 M. K. O'Reilly and J. C. Paulson, *Methods Enzymol.*, 2010, **478**, 343–363.

81 A. P. May, R. C. Robinson, M. Vinson, P. R. Crocker and E. Y. Jones, *Mol. Cell*, 1998, **1**, 719–728.

82 P. R. Crocker, M. Vinson and S. Kelm, *Biochem. J.*, 1999, **341**, 355–361.

83 (*a*) H. Prescher, M. Frank, S. Gütgemann, E. Kuhfeldt, A. Schweizer, L. Nitschke, C. Watz and R. Brossmer, *J. Med. Chem.*, 2017, **60**, 941–956; (*b*) M. Frank, E. Kuhfeldt, J. Cramer, C. Watzl and H. Prescher, *J. Med. Chem.*, 2023, **66**, 14315–14334.

84 H. Prescher, A. Schweizer, E. Kuhfeldt, L. Nitschke and R. Brossmer, *ACS Chem. Biol.*, 2014, **9**, 1444–1450.

85 (*a*) H. Tateno, P. R. Crocker and J. C. Paulson, *Glycobiology*, 2005, **15**, 1125–1135; (*b*) B. S. Bochner, R. A. Alvarez, P. Mehta, N. V. Bovin, O. Blixt, J. R. White and R. L. Schnaar, *J. Biol. Chem.*, 2005, **280**, 4307–4312.

86 J. M. Pröpster, F. Yang, S. Rabbani, B. Ernst, F. H. T. Allain and M. Schubert, *Proc. Natl. Acad. Sci. U. S. A.*, 2016, **113**, E4170–E4179.

87 M. P. Lenza, U. Atxabal, C. Nycholat, I. Oyenarte, A. Franconetti, J. I. Quintana, S. Delgado, R. Núñez-Franco,

This journal is © The Royal Society of Chemistry 2024

Chem. Soc. Rev., 2024, **53**, 9428–9445 | **9443**

C. T. G. Marroquín, H. Coelho, L. Unione, G. Jiménez-Oses, F. Marcelo, M. Schubert, J. C. Paulson, J. Jiménez-Barbero and J. Ereño-Orbea, *JACS Au*, 2023, **3**, 204–215.

88 (a) C. M. Nycholat, S. Duan, E. Knuplez, C. Worth, M. Elich, A. Yao, J. O'Sullivan, R. McBride, Y. Wei, S. M. Fernandes, Z. Zhu, R. L. Schnaar, B. S. Bochner and J. C. Paulson, *J. Am. Chem. Soc.*, 2019, **141**, 14032–14037; (b) B. S. Kroezen, G. Conti, B. Girardi, J. Cramer, X. Jiang, S. Rabbani, J. Müller, M. Kokot, E. Luisoni, D. Ricklin, O. Schwardt and B. Ernst, *ChemMedChem*, 2020, **15**, 1706–1719.

89 G. Conti, A. Bärenwaldt, S. Rabbani, T. Mühlethaler, M. Sarcevic, X. Jiang, O. Schwardt, D. Ricklin, R. J. Pieters, H. Läubli and B. Ernst, *Angew. Chem., Int. Ed.*, 2023, **62**, e202314280.

90 J. J. Lundquist and E. J. Toone, *Chem. Rev.*, 2002, **102**, 555–578.

91 Y. C. Lee and R. T. Lee, *Acc. Chem. Res.*, 1995, **8**, 321–327.

92 M. Mammen, S. K. Choi and G. M. Whitesides, *Angew. Chem., Int. Ed.*, 1998, **37**, 2754–2794.

93 (a) T. K. Dam, R. Roy, D. Pagé and C. F. Brewer, *Biochemistry*, 2002, **41**, 1351–1358; (b) T. K. Dam, T. A. Gerken and C. F. Brewer, *Biochemistry*, 2009, **48**, 3822–3827.

94 L. R. Olsen, A. Dessen, D. Gupta, S. Sabesan and J. Sacchettini, *Biochemistry*, 1997, **36**, 15073–15080.

95 K. E. Pace, C. Lee, P. L. Stewart and L. G. Baum, *J. Immunol.*, 1999, **163**, 3801–3811.

96 M. Abbas, M. Maalej, F. Nieto-Fabregat, M. Thépaut, J. P. Kleman, I. Ayala, A. Molinaro, J. P. Simorre, R. Marchetti, F. Fieschi and C. Laguri, *PNAS Nexus*, 2023, **2**, 1–10.

97 K. L. Hudson, G. J. Bartlett, R. C. Diehl, J. Agirre, T. Gallagher, L. L. Kiessling and D. N. Woolfson, *J. Am. Chem. Soc.*, 2015, **137**, 15152–15160.

98 A. Gabba, A. Bogucka, J. G. Luz, A. Diniz, H. Coelho, F. Corzana, F. J. Cañada, F. Marcelo, P. V. Murphy and G. Birrane, *Biochemistry*, 2021, **60**, 1327–1336.

99 F. Marcelo, F. Garcia-Martin, T. Matsushita, J. Sardinha, H. Coelho, A. Oude-Vrielink, C. Koller, S. Andre, E. J. Cabrita, H. J. Gabius, S. I. Nishimura, J. Jimenez-Barbero and J. Canada, *Chem. – Eur. J.*, 2014, **20**, 16147–16155.

100 M. Sakakura, S. Oo-Puthinan, C. Moriyama, T. Kimura, J. Moriya, T. Irimura and I. Shimada, *J. Biol. Chem.*, 2008, **283**, 33665–33673.

101 D. M. Beckwith, F. G. FitzGerald, M. C. Rodriguez Benavente, E. R. Mercer, A. K. Ludwig, M. Michalak, H. Kaltner, J. Kopitz, H. J. Gabius and M. Cudic, *Biochemistry*, 2021, **60**, 547–558.

102 S. André, S. O'Sullivan, C. Koller, P. V. Murphy and H. J. Gabius, *Org. Biomol. Chem.*, 2015, **13**, 4190.

103 H. Kaltner, J. C. Manning, G. G. Caballero, C. Di Salvo, A. Gabba, L. L. Romero-Hernández, C. Knospe, D. Wu, H. C. Daly, D. F. O'Shea, H. J. Gabius and P. V. Murphy, *RSC Adv.*, 2018, **8**, 28716–28735.

104 A. Gabba, R. Attariya, S. Behren, C. Pett, J. C. van der Horst, H. Yurugi, J. Yu, M. Urschbach, J. Sabin, G. Birrane,

E. Schmitt, S. J. van Vliet, P. Besenius, U. Westerlind and P. V. Murphy, *J. Am. Chem. Soc.*, 2023, **145**, 13027–13037.

105 N. K. Sauter, J. E. Hanson, G. D. Glick, J. H. Brown, R. L. Crowther, S. J. Park, J. J. Skehel and D. C. Wiley, *Biochemistry*, 1992, **31**, 9609–9621.

106 R. U. Kadam and I. A. Wilson, *Proc. Natl. Acad. Sci. U. S. A.*, 2018, **115**, 4240–4245.

107 A. J. Thompson and J. C. Paulson, *J. Biol. Chem.*, 2021, **296**, 100017.

108 Y. Ji, Y. J. B. White, J. A. Hadden, O. C. Grant and R. J. Woods, *Curr. Opin. Struct. Biol.*, 2017, **44**, 219–231.

109 (a) X. Xiong, P. Coombs, S. Martin, J. Liu, H. Xiao, J. W. McCauley, K. Locher, P. A. Walker, P. J. Collins, Y. Kawaoka, J. J. Skehel and S. J. Gamblin, *Nature*, 2013, **497**, 392–396; (b) N. K. Sauter, M. D. Bednarski, B. A. Wurzburg, J. E. Hanson, G. M. Whitesides, J. J. Skehel and D. C. Wiley, *Biochemistry*, 1989, **28**, 8388–8396.

110 W. Peng, R. P. de Vries, O. C. Grant, A. J. Thompson, R. McBride, B. Tsogtbaatar, P. S. Lee, N. Razi, I. A. Wilson, R. J. Woods and J. C. Paulson, *Cell Host Microbe*, 2017, **21**, 23–34.

111 K. J. Taubenberger and J. C. Kash, *Cell Host Microbe*, 2010, **7**, 440–451.

112 W. Lu, W. Du, V. J. Somovilla, G. Yu, D. Haksar, E. de Vries, G. J. Boons, R. P. de Vries, C. A. M. de Haan and R. J. Pieters, *J. Med. Chem.*, 2019, **62**, 6398–6404.

113 G. Bachem, E. C. Wamhoff, K. Silberreis, D. Kim, H. Baukmann, F. Fuchsberger, J. Dernedde, C. Rademacher and O. Seitz, *Angew. Chem., Int. Ed.*, 2020, **59**, 21016–21022.

114 S. Ordanini, N. Varga, V. Porkolab, M. Thepaut, L. Belvisi, A. Bertaglia, A. Palmioli, A. Berzi, D. Trabattoni, M. Clerici, F. Fieschi and A. Bernardi, *Chem. Commun.*, 2015, **51**, 3816–3819.

115 G. Tabarani, M. Thepaut, D. Stroebel, C. Ebel, C. Vives, P. Vachette, D. Durand and F. Fieschi, *J. Biol. Chem.*, 2009, **284**, 21229–21240.

116 (a) V. Porkolab, C. Pifferi, I. Sutkeviciute, S. Ordanini, M. Taouai, M. Thépaut, C. Vivès, M. Benazza, A. Bernardi, O. Renaudet and F. Fieschi, *Org. Biomol. Chem.*, 2020, **18**, 4763–4772; (b) V. Porkolab, M. Lepšík, S. Ordanini, A. St John, A. Le Roy, M. Thépaut, E. Paci, C. Ebel, A. Bernardi and F. Fieschi, *ACS Cent. Sci.*, 2023, **9**, 709–718.

117 R. Visini, X. Jin, M. Bergmann, G. Michaud, F. Pertici, O. Fu, A. Pukin, T. R. Branson, D. M. E. Thies-Weesie, J. Kemmink, E. Gillon, A. Imberty, A. Stocker, T. Darbre, R. J. Pieters and J. L. Reymond, *ACS Chem. Biol.*, 2015, **10**, 2455–2462.

118 P. Rohse, S. Weickert, M. Drescher and V. Wittmann, *Chem. Sci.*, 2020, **11**, 5227–5237.

119 L. M. Luh, U. Scheib, K. Juenemann, L. Wortmann, M. Brands and P. M. Cromm, *Angew. Chem., Int. Ed.*, 2020, **59**, 15448–15466.

120 S. M. Banik, K. Pedram, S. Wisnovsky, G. Ahn, N. M. Riley and C. R. Bertozzi, *Nature*, 2020, **584**, 291–297.

121 Y. Zhou, P. Teng, N. T. Montgomery, X. Li and W. Tang, *ACS Cent. Sci.*, 2021, **7**, 499–506.

9444 | *Chem. Soc. Rev.*, 2024, **53**, 9428–9445

This journal is © The Royal Society of Chemistry 2024

122 T. P. Prakash, M. J. Graham, J. Yu, R. Carty, A. Low, A. Chappell, K. Schmidt, C. Zhao, M. Aghajan, H. F. Murray, S. Riney, S. L. Booten, S. F. Murray, H. Gaus, J. Crosby, W. F. Lima, S. Guo, B. P. Monia, E. E. Swayze and P. P. Seth, *Nucleic Acids Res.*, 2014, **42**, 8796–8807.

123 V. Kumar and W. B. Turnbull, *Chem. Soc. Rev.*, 2023, **52**, 1273–1287.

124 E. A. L. Biessen and T. J. C. van Berkel, *Arterioscler., Thromb., Vasc. Biol.*, 2021, **41**, 2855–2865.

125 D. M. Bissell, K. E. Anderson and H. L. Bonkovsky, *N. Engl. J. Med.*, 2017, **377**, 862–872.

126 N. H. Gosselin, V. J. A. Schuck, O. Barriere, K. Kulmatycki, A. Margolskee, P. Smith and Y. He, *Clin. Pharmacol. Ther.*, 2023, **113**, 328–338.

127 A. Mishra, T. R. Castañeda, E. Bader, B. Elshorst, S. Cummings, P. Scherer, D. S. Bangari, C. Loewe, H. Schreuder, C. Pöverlein, M. Helms, S. Jones, G. Zech, T. Licher, M. Wagner, M. Schudok, M. deHoop, A. T. Plowright, J. Atzrodt, A. Kannt, I. Laitinen and V. Derdau, *Adv. Sci.*, 2020, **7**, 2002997.

128 K. Wojtczak, E. Zahorska, I. J. Murphy, F. Koppel, G. Cooke, A. Titz and J. P. Byrne, *Chem. Commun.*, 2023, **59**, 8384–8387.

129 K. N. Kirschner, A. B. Yongye, S. M. Tschampel, C. R. Daniels, B. L. Foley and R. J. Woods, *J. Comput. Chem.*, 2008, **29**, 622–655.

130 J. H. Lee, G. Ozorowski and A. B. Ward, *Science*, 2016, **351**, 1043–1048.

131 J. Jumper, R. Evans, A. Pritzel, T. Green, M. Figurnov, O. Ronneberger, K. Tunyasuvunakool, R. Bates, A. Žídek, A. Potapenko, A. Bridgland, C. Meyer, S. A. A. Kohl, A. J. Ballard, A. Cowie, B. Romera-Paredes, S. Nikolov, R. Jain, J. Adler, T. Back, S. Petersen, D. Reiman, E. Clancy, M. Zielinski, M. Steinegger, M. Pacholska, T. Berghammer, S. Bodenstein, D. Silver, O. Vinyals, A. W. Senior, K. Kavukcuoglu, P. Kohli and D. Hassabis, *Nature*, 2021, **596**, 583–589.

132 A. Gabba, P. V. Murphy, L. L. Kiessling and G. Birrane, *Biochemistry*, 2024, **63**, 191–193.

133 L. Mousavifar and R. Roy, *Drug Discovery Today*, 2021, **26**, 2124–2137.

134 E. Zahorska, F. Rosato, K. Stober, S. Kuhaudomlarp, J. Meiers, D. Hauck, D. Reith, E. Gillon, K. Rox, A. Imberty, W. Römer and A. Titz, *Angew. Chem., Int. Ed.*, 2023, **6**, e202215535.

135 R. Sommer, S. Wagner, K. Rox, A. Varrot, D. Hauck, E.-C. Wamhoff, J. Schreiber, T. Ryckmans, T. Brunner, C. Rademacher, R. W. Hartmann, M. Brönstrup, A. Imberty and A. Titz, *J. Am. Chem. Soc.*, 2018, **140**(7), 2537–2545.

136 M. Egli and M. Manoharan, *Nucleic Acids Res.*, 2023, **51**, 2529–2573.